JOURNAL OF
LIPID SCIENCE AND TECHNOLOGY

1945 2005
In Pursuit of Excellence

FARELABS

FOOD ANALYSIS & RESEARCH LABORATORY

A commitment for a better tomorrow

Research and Development

Excellence
Creative industry oriented solutions

Founded in 1999, FARE Labs Private Limited is a leading NABL accredited, FSSAI authorised & MOEF recognised laboratory institution of India. It is based in Gurgaon, and is promoted by Dwijendra Mathur and Chandra Shekar Joshi, a team of chemical engineers with a combined industry work experience of over 51 years.

Analytical Testing

Accuracy
Attention to detail

FARE Labs possesses world-class competencies in Analytical Testing and Research & Development. In addition, it also has a strong Consultancy and Training division to provide holistic solutions to its clients.

Credentials

Trustworthiness
Successful business relationships

Consultancy and Training

Reliability
Abundant & diverse experience

Water, Fuels & bio-fuels
Food & Agriculture
Fats, Oils & Allied products
Pollution & Environment
Essential Oils, Herbs & Cosmetics
Soaps, Detergents & Toiletries
Packing material, Petrolium & Lubricants
Industrial & Fine Chemicals
Wood Testing & Soil Strength

FARE LABS Private Limited
L-17/3, DLF Phase-II, IFFCO Chowk, M. G. Road, Gurgaon-122002, Haryana, INDIA.
Phone : +91-124-4223207-08, 4034205, Fax : +91-124-4036038, Cell : +91-93126 64533
Email : farelabs@farelabs.com, Website : www.farelabs.com

Journal of Lipid Science and Technology

CONTENTS

प्रकृति से पकवानों तक

बैल कोल्हू®

• कच्ची घानी सरसों का तेल • रिफाइंड ऑयल्स
• चना बेसन

लाजवाब स्वाद, बेजोड़ शुद्धता

From Editors Desk

Import of refined bleached and deodorized palm oil is affecting India badly. India has started importing palm stearin, a byproduct of crude palm oil processing which is hurting Indian crushers. The less duty differential between CPO & CPS is hurting Indian industry. If we have to increase farmer's income we must increase the duty on both CPO & RBD but duty differential must be at least 15% (i.e., CPO should fetch 15% lower duty than RBD so that Indian farmer gets better price for the crop as well as refiners and crushers are able to utilize its production capacity to a better extent.

The rising gap in India between the domestic production of oils and import of oils putting pressure on trade deficit as well as food security. The government of India has to come out with a time-bounded action plan to minimize the dependence on imported edible oils. Oilseeds are not only important source of edible oils but are a vital source of protein to for human as well as animal nutrition. Therefore, it needs a serious intervention by government to reduce dependency on imported oils by encouraging local produce and increasing MSP of oilseeds as well as producing high yielding variety of oilseeds. Further, research and development be encouraged in agriculture university for identifying high yielding varieties so as we are near to as par with the world standards. Further, developed nations like (USA, Brazil, etc.) are now-a-days relying.

GMO-Crop which gives higher yields and there is no need of horizontal expansion of land.

(R.P. SINGH)

INDEX TO ADVERTISEMENTS / ANNOUNCEMENTS

Sorbitan Esters (SPANs) as Stabilizers for Silver Nanoparticles in Microemulsion Mediated Synthesis

Prateek Shukla[a*], Tandra Nandi [b] and Rajinder Pal Singh[c]

[a] Department of Chemistry, Indian Institute of Technology, Kanpur- 208016, India
[b] Defence Materials and Stores Research and Development Establishment (DRDO)
[c] Rohilkhand Laboratory and Research Centre, Bareilly - 243502, India

Corresponding author E-mail : prateek.shukla8@gmail.com

Abstract:

Sorbitan esters (spans) due to their distinguished properties like emulsifiers and wetting agents were employed as capping agents during synthesis of silver nanoparticles via microemulsion method. Syntheses of silver nanoparticles were accomplished by a chemical reduction reaction in a microemulsion media, formed under high shear mixing condition. Aqueous silver nitrate solution was used as a source of silver ions, 2-ethyl hexanol as oil phase and an aqueous solution of sodium borohydride was used as reducing agent. Different sorbitan esters like sorbitan monostearate (span 60), sorbitan tristearate (span 65), sorbitan monooleate (span 80) and sorbitan trioleate (span 85) were employed as capping agents for silver nanoparticles during synthesis and their effect on size and shape of silver nanoparticles is studied. Transmission electron microscopy (TEM) and dynamic light scattering (DLS) techniques were used for elucidating the shape, size and size distribution of the synthesized silver nanoparticles. Crystal structure of silver nanoparticles thus prepared has been studied by X-ray diffraction analysis (XRD). UV-Vis technique was used to study surface plasmon resonance (SPR) of the synthesized silver nanoparticles. The results of synthesis of silver nanoparticles in the present study were excellent and may be utilized at a higher scale.

1. Introduction

Many researchers have given a great interest in the synthesis of different metal nanoparticles with controllable particle size distribution. Due to unusual properties of nanostructured silver particles, these nanoparticles have been subjected to numerous researchers. In comparison with larger size particles, nanoparticles exhibit newer and improved properties like higher surface to volume ratio, changes in total energy, changes in conductivity, different optical features) 1. Therefore to prepare silver nanoparticles with specific nano size and monodispersity has become a challenge in the research area in recent years. Many methods have been exploited by various researchers for the synthesis of silver nanoparticles in the past few years; wherein the chemical reaction in the microemulsion is one of the most important methods for synthesis of monodisperse nanoparticles 2.

Synthesis of nanoparticles via chemical reduction method could be considered suitable for the bulk synthesis of nanoparticles in a relatively shorter period of time 3. A typical synthesis of silver nanoparticles by chemical reduction process involved three main stages:

i.   Reduction
ii.   Growth and
iii.   Protection

The first one is the reduction of a silver salt is carried out by a reducing agent. AgNO3 is most frequently used as a source of silver ions due to its higher solubility in aqueous solution and NaBH4 as a reducing agent. In the second stage, newly generated neutral silver atoms collide with each other, forming stable nuclei and a growth of the nanoparticle occurs until all metals ions are consumed. In the final stage prevention of agglomeration of nanoparticles is achieved by the suitable protecting agents or capping agents. Stabilizers interact with small particles to prevent their agglomeration via adsorption at their outer surface4, 5. Moreover, chemical reduction methods were advantageous as morphology (i.e. diameter, size distribution, shape) of nanostructured silver nanoparticles could be controlled by various reaction parameters. The important key to this approach is to prevent the agglomeration of silver nanoparticles during the course of synthesis procedures. Generally, special organic compounds called surfactants with specific hydrophilic-lipophilic balance (HLB) value were used for the purpose. The microdroplets in the microemulsion could be in the form of oil-swollen micelles dispersed in an aqueous phase as o/w microemulsion or water-swollen micelles dispersed in oil phase as w/o microemulsion 6, 7, 8, 9.

Spontaneous emulsification under high-shear mixing, high-pressure homogenization or ultrasonification was less expensive and energy efficient alternatives that utilize the chemical energy stored in the microemulsion system. High energy methods were effective in reducing droplet size and with the aid of proper stabilizers. Surfactants could be employed effectively for the synthesis of different nanoparticles 10, 11, 12.In past studies generally, hydrazine, sodium borohydride, ascorbic acid etc were used as the reducing agents and sodium dodecyl sulfate, cetyltrimethylammonium bromide, poly (vinyl alcohol), poly (vinylpyrrolidone), is used as the reducing- and stabilizing-agents respectively to prepare silver nanoparticles with controlled size and shape 13.

Sorbitan esters are commercially supplied as Spans (non-ionic surfactants). They are generally insoluble in water (low HLB) and are used as water in oil emulsifiers and wetting agents. Their molecules have no charge insolvent but normally consist of a highly polar region such as hydroxyl groups. At low concentrations, these surfactant molecules are present as un-associated monomers. As the surfactant concentration is increased, both the attractive and repulsive forces among the molecules cause self-aggregation to occur resulting in the formation of micelles. The concentration at which these

micelles formation takes place is called the critical micelle concentration (CMC). The characteristics of these micelles can be controlled by small changes in the chemical structure of the surfactant molecules or by varying the conditions of the dispersing phase. Changes in the pH, ionic strength and temperature are all known to influence the size and shape of surfactant micelles. In some cases, the micelle size can be affected by the concentration of surfactant14-21.

In the present paper, we have discussed the synthesis of silver nanoparticles using high energy microemulsion method using different capping agents. Silver nitrate was used as a silver ion source in aqueous media, sodium borohydride as reducing agent, and 2- ethyl hexanol as the organic phase. Different sorbitan esters (fig-1) like sorbitan monostearate (span 60) of HLB-4.7, sorbitan tristearate (span 65) of HLB-2.1, sorbitan monooleate (span 80) of HLB-4.3 and sorbitan trioleate (span 85) of HLB-1.8, were employed as capping agents for silver nanoparticles. Transmission electron microscopy (TEM) and dynamic light scattering (DLS) techniques were used for elucidating the shape, size and size distribution of the synthesized silver nanoparticles. Crystal structure of silver nanoparticles thus prepared has been studied by X-ray diffraction analysis (XRD). UV-Vis technique was used to study surface plasmon resonance (SPR) of the synthesized silver nanoparticles.
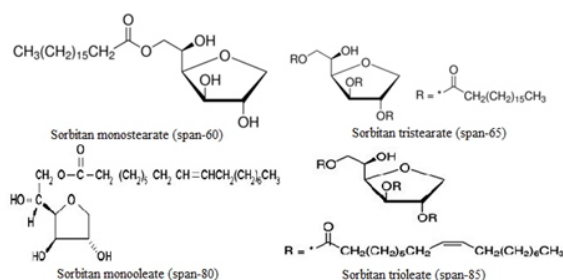

Figure : Structure of different sorbitan esters.

2. Materials and method

A synthetic method developed for the purpose of this experiment enables the production of stable silver nanoparticles under an optimized set of conditions. The silver nitrate ($\geqslant$99.0%, AgNO3) and sodium borohydride ($\geqslant$ 96.0%, NaBH4) were purchased from Sigma-Aldrich and Merck chemicals respectively. Different sorbitan esters like sorbitan monostearate (span 60) of HLB-4.7, sorbitan tristearate (span 65) of HLB-2.1, sorbitan monooleate (span 80) of HLB-4.3 and sorbitan trioleate (span 85) of HLB-1.8, an organic solvent 2-ethyl hexanol were purchased from Fluka chemicals. All chemicals were used without further purification. Double distilled water was used for the preparation of all samples.

2.1. Synthesis of Silver Nanoparticles

Synthesis of silver nanoparticles by chemical reduction method using silver nitrate as a source of silver ion and sodium borohydride as reducing agent have been used by many researchers. However, fewer claimed their work suitable for bulk synthesis with controlled particle size distribution. A. Katiyaret al. has reported the synthesis of Fe-Ni nanoparticles with controlled morphology for preparing magnetic nanofluid 15. In our present study, spans stabilized spherical silver nanoparticles were synthesized via forming a microemulsion by high energy methods 16. Here microemulsion is formed by mixing bulk amount (250 ml) of aqueous silver nitrate solution (as water phase), 2-ethyl hexanol (as oil phase) and different sorbitan esters as a surfactant. Different sorbitan esters like sorbitan monostearate (span 60) of HLB-4.7, sorbitan tristearate (span 65) of HLB-2.1, sorbitan monooleate (span 80) of HLB-4.3 and sorbitan trioleate (span 85) of HLB-1.8 were used separately as capping agents in the different set of reactions. IKA T25 digital ultra turrax, a high-speed homogenizer was used to homogenize all components at a speed of 22000 rpm in a vessel and temperature is maintained at 400C in a water bath. An aqueous solution of sodium borohydride was added dropwise to the mixture under high shear mixing conditions. A spontaneous reduction reaction occurred due to exothermic nature of the reaction. Formation of black colloidal suspension reveals the formation of silver nanoparticles.

2.2. Characterization of silver nanoparticles

Silver nanoparticles prepared as above were characterized for their surface morphology along with SAD (selected area diffraction) pattern by TEM analysis by FEI Tecnai- G2 F20 (X-TWIN) transmission electron microscope using Cu-grid 200 mesh (Ted Pella INC.). Figure 2 and 3 shows TEM image and SAD pattern of silver nanoparticles synthesized by using different span capping agents. Perfect nano-crystalline nature was observed in SAD patterns of silver nanoparticles synthesized by using different span capping agents. Particle size distribution was taken with the help of Malvern Zeta sizer ZS90 instrument (Figure 2 and 3). XRD analysis of silver nanoparticles was done by X-ray diffractometer; model ISO Debyeflex 2002 (Figure 4). Optical properties of silver nanoparticles were studied by JASCO V-630 Spectrophotometer (Figure 5 and 6).

3. Results and Discussions

3.1 Effect of spans on silver nanoparticles

Different sorbitan esters like sorbitan monostearate (span 60) of HLB-4.7, sorbitan tristearate (span 65) of HLB-2.1, sorbitan monooleate (span 80) of HLB-4.3 and sorbitan trioleate (span 85) of HLB-1.8 were used successfully as capping agents in four sets of reactions separately. All four syntheses of silver nanoparticles were performed by taking a constant amount capping agent (4.5 mmol) each time. Figure-2 shows TEM image and SAD pattern of silver nanoparticles synthesized by using span-60 and span 65 capping agents. The average particle hydrodynamic diameter as determined by dynamic light scattering technique (DLS) was found as about

50 nm for span-60 stabilized silver nanoparticles which was further decreased to about 40 nm for span-65 stabilized silver nanoparticles. Since light scattering techniques measure the hydrodynamic diameter, the actual diameters of nanoparticles were always found less than the reported ones. The hydrodynamic diameter for span-80 stabilized silver nanoparticles was found as about 40 nm and for span-85 stabilized silver nanoparticles it was further decreased to about 30 nm (figure-3).

For the most surfactant-mediated synthesis, the connection between the morphology of the surfactant aggregates and the resulting particle structure is more complex than simply relating the average size and shape of the micelles to the size and shape of the precipitated

particles. In both the set of experiments (1) span-60 vs. Span-65 and (2) span-80 vs. Span-85, a decrease in average particle diameter is noticed which might be due to a decrease in relative HLB of capping agents used. Capping agents (spans) got adsorbed on the oil/water interphase depending upon their structure. Adsorption and stabilization were found to be most effective when the surfactant is more soluble in the continuous phase, i.e. for W/O emulsions, an oil-soluble surfactant (low HLB) is most efficient.

The span surfactants consist of two main entities, a hydrophilic head group and a hydrophobic (or lipophilic) tail group (figure-1), which form soft aggregates in 2- ethyl hexanol (oil phase) and are held together by Vander Waals and ionic forces. The span surfactant acts as a stabilizing agent, effectively dispersing the obtained silver nanoparticles in the solution, providing sites for the particle nucleation and preventing aggregation of the newly generated silver nanoparticles. In W/O microemulsions span surfactants form reverse micelles, nano-sized water pools dispersed within the bulk organic solvent (2-ethyl hexanol) which acts as nanoreactors for the chemical reduction of the metallic precursors (aqueous silver nitrate solution) and metallic silver nanoparticle preparation. The packing of span capping agents at the oil-water interface played a key role in controlling the size and shape of silver nanoparticles during microemulsion mediated synthesis. The packing parameters of span surfactants or capping agents depend upon the relative sizes of the hydrophilic, and the hydrophobic group. The effective hydrophilic group is not the size of the molecule, but rather the effect of surfactant solutions of the charge if ionic. The effective size of the hydrophobic group will depend on whether the alkyl chain is linear or branched, or whether there are one, two or more hydrophobic chains. It was well noticed in our synthesisthat such variations in the alkyl chain give practical differences in the use of the surfactant or capping agent.
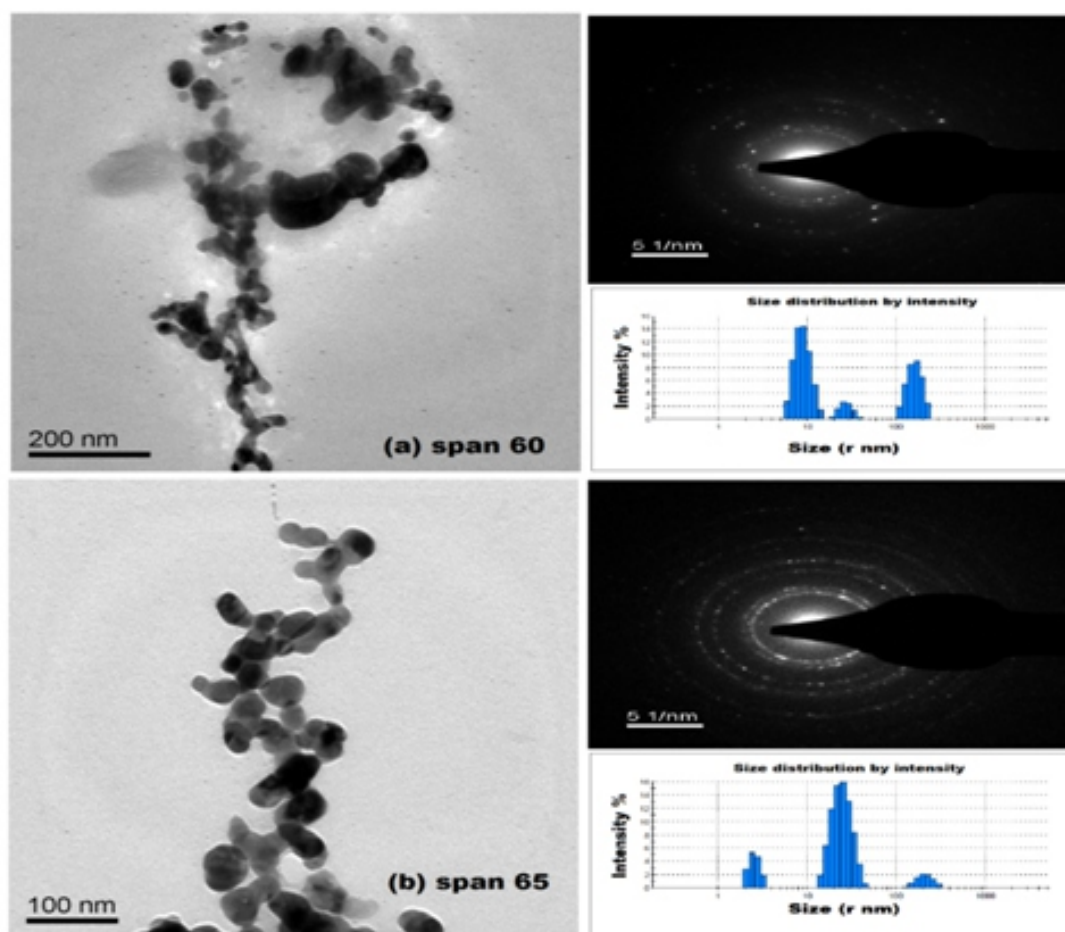
Figure 2 : TEM image, SAD pattern and particle size distribution of silver nanoparticles synthesized by using (a) span 60 and (b) span 65 as capping agents.
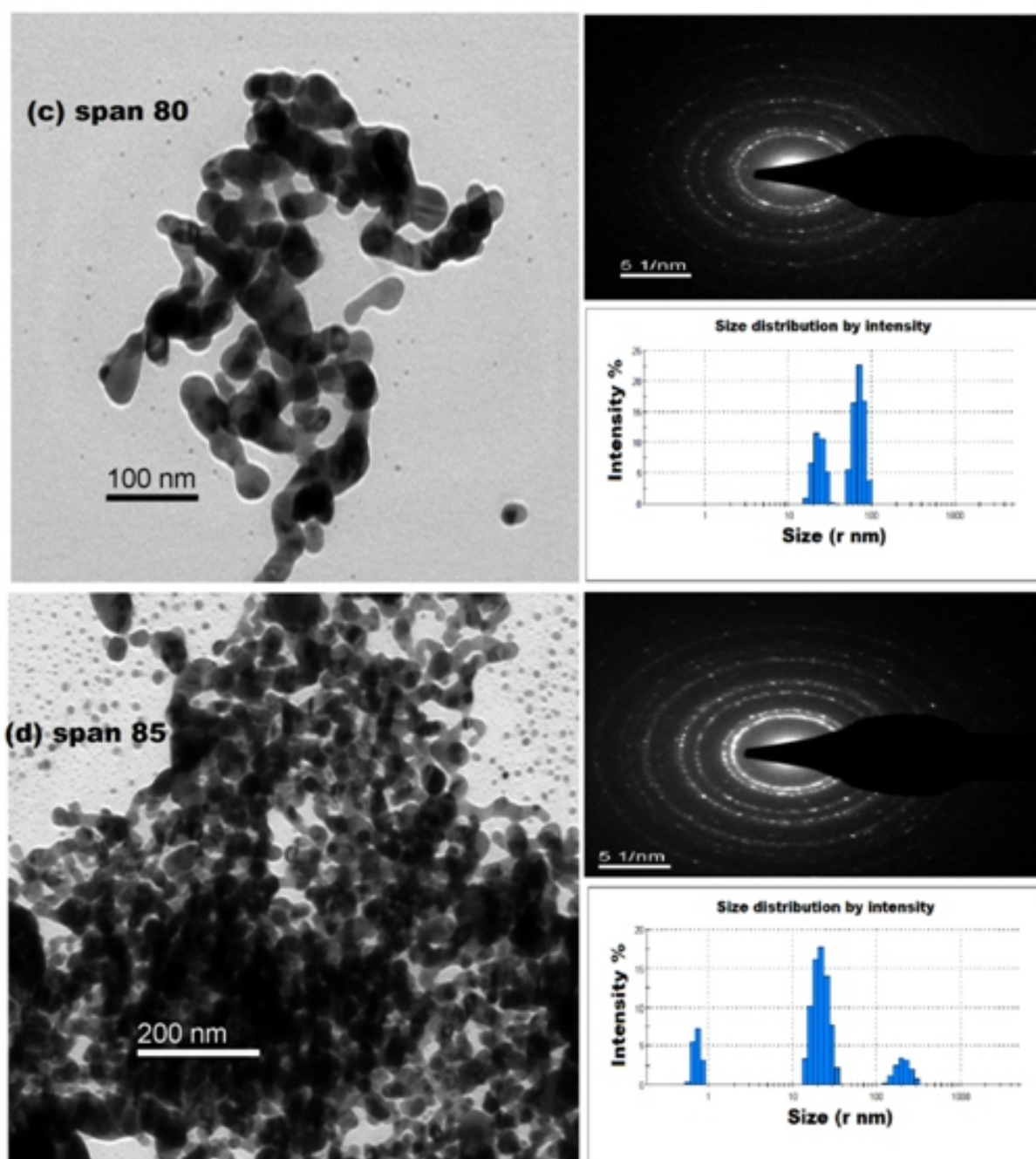
Figure 3 : TEM image, SAD pattern and particle size distribution of silver nanoparticles synthesized by using (a) span 80 and (b) span 85 as capping agents

3.2 X-ray diffraction study of silver nanoparticles

A typical XRD pattern of the silver nanoparticles prepared by using different span capping agents is shown in figure 4. The X-ray powder diffraction (XRD) pattern was recorded with Cu Kα radiation (λ= 1.54184 A0) in 2-theta ranging from 100 to 900 with the scan speed of 30/min. Here, the Bragg's reflections observed at 2-theta values of 38.115, 44.229, 64.443, 77.397 and 81.541 representing [111], [200], [220], [311] and [222] planes respectively; which indicate the formation of silver nanocrystals with cubic face centered (FCC) structure in all set of experiment. The peaks obtained are consistent with JCPDS card no. 87-0597. Absences of any other peaks indicate the purity of synthesized silver nanoparticles.
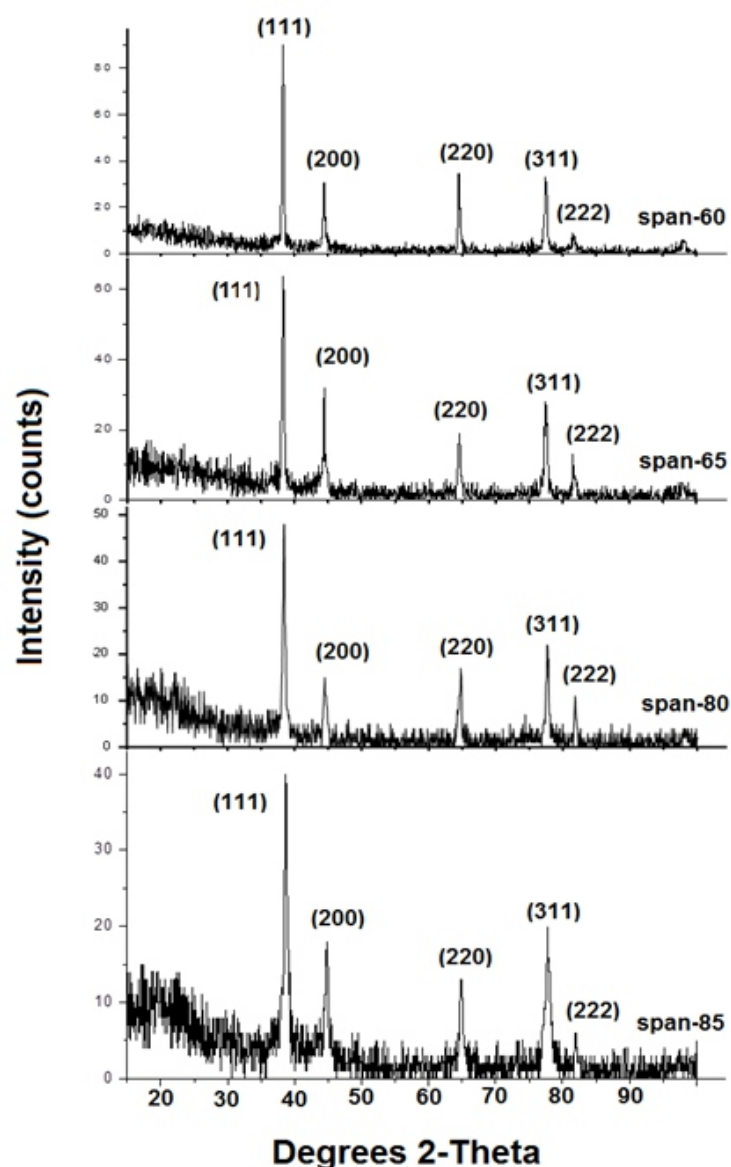
Figure 4: XRD pattern of nanoparticles synthesized by using different capping agents

3.3 Optical properties of silver nanoparticles

Due to localized surface Plasmon resonance (LSPR), silver nanoparticles have remarkable optical properties which are a function of the size, shape, surfactant coating and medium of suspension. The optical properties of silver nanospheres are highly dependent the diameter of nanoparticles. All the analysis of LSPR for silver nanoparticles was carried out by making their dispersions in heptane. Ultrasonic processor (Vibracell Model VCX 750, Sonics & Materials INC, USA) was used for uniform dispersions. Figure-5 shows the relative absorbance of silver nanoparticles synthesized by using span-60, span-65, span-80 and span-85 capping agents. With the increase in the size of silver nanoparticles, their unique Plasmon band shifts towards the red region of the visible spectrum. Smaller size silver nanoparticles are primarily absorbing and have a clear light yellow color solution in heptanes. Figure-6 shows the relative absorbance of silver nanoparticles synthesized by using span-85 capping agent at different time intervals ranging from 1 to 10 hr. It has been observed that as the silver nanoparticles get larger in size, the scattering portion of the extinction increased. This increase in the scattering component resulted in the solution becoming darker in color and finally become gray in color. This unique LSPR phenomenon of plasmonic silver nanoparticles provides an easy and consistent way to monitor the stability of silver nanoparticle dispersions. When dispersions of silver nanoparticles become destabilized and agglomerated, the visible spectra will change. There will be a drop in intensity, broadening of the curve and sometimes a secondary peak will observe at a longer wavelength.
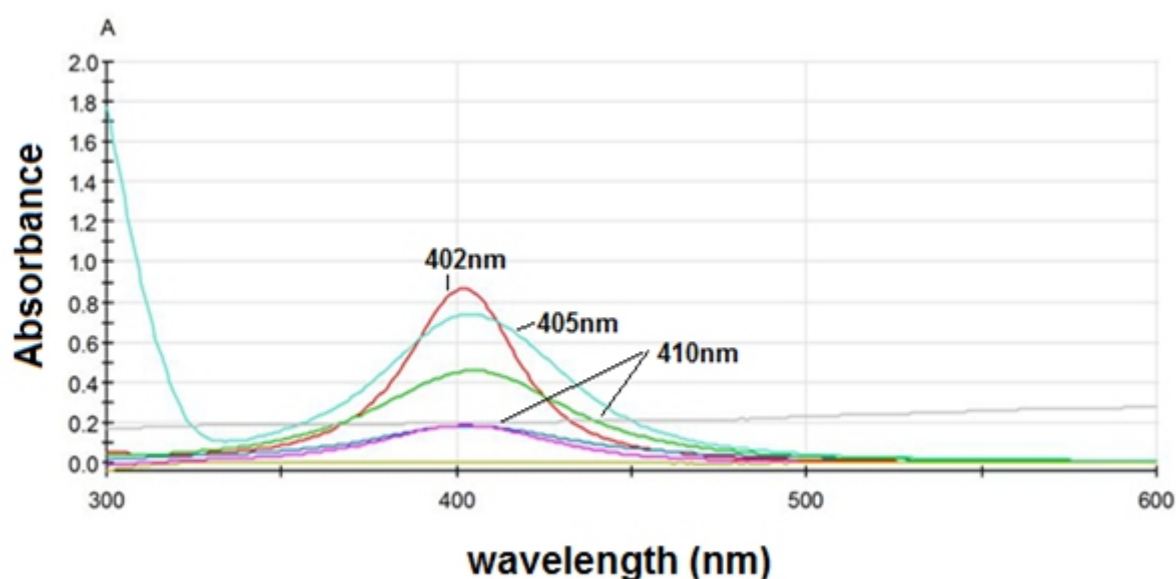
Figure 5: UV-Vis spectra of silver nanoparticles synthesized by using different span capping agents.
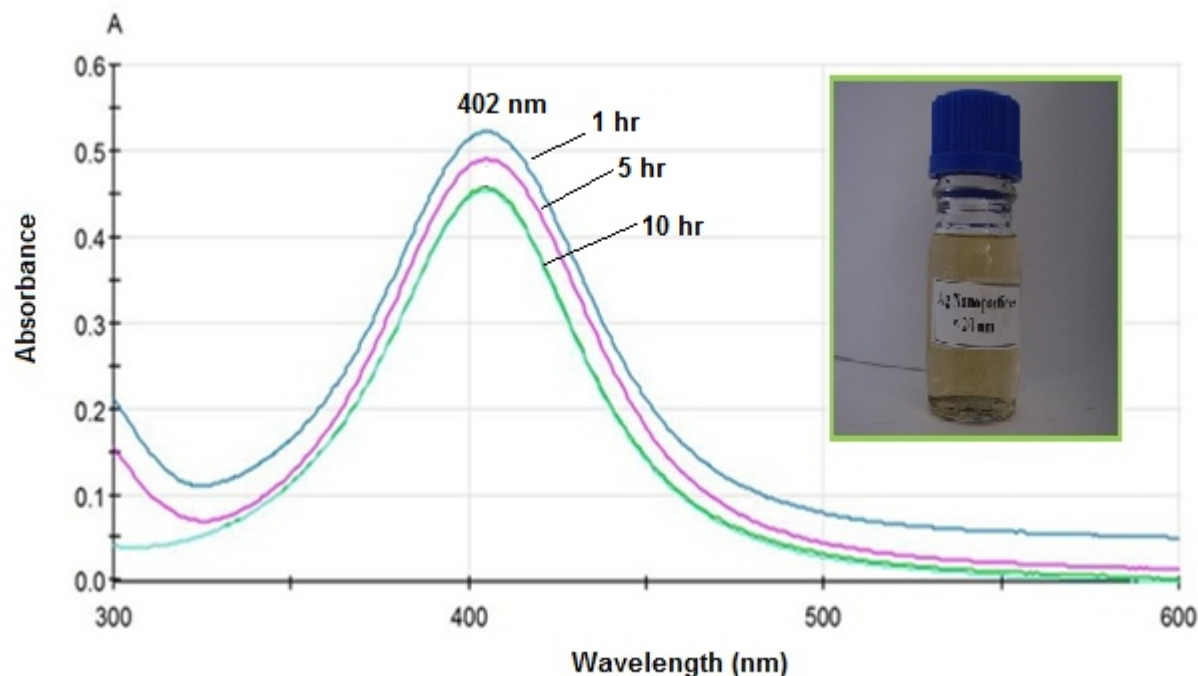
Figure 6:UV-Vis spectra of silver nanoparticles synthesized by span 85 capping agents at different time intervals.

4. Conclusion

Silver nanoparticles with uniform particle size distribution were successfully synthesized by carrying out a chemical reduction reaction in a microemulsion media, prepared under high shear mixing conditions. An aqueous solution of silver nitrate was taken as a silver ion source, sodium borohydride as reducing agent, 2- ethyl hexanol as organic phase and spans as stabilizers. Different sorbitan esters like sorbitan monostearate (span 60) of HLB-4.7, sorbitan tristearate (span 65) of HLB-2.1, sorbitan monooleate (span 80) of HLB-4.3 and sorbitan trioleate (span 85) of HLB-1.8 were used successfully as capping agents in four sets of reactions separately. In both the set of experiments (1) span-60 vs. Span-65 and (2) span-80 vs. Span-85, a decrease in average particle diameter is noticed which might be due to a decrease in relative HLB of capping agents used.The synthesized silver nanoparticles were successfully characterized via TEM and DLS analysis for their size, shape and size distribution. XRD analysis showed their good crystalline nature. Well, localized

surface Plasmon resonance of synthesized silver nanoparticles is observed and it has been observed that as the silver nanoparticles get larger in size, the scattering portion of the extinction increased. Thus silver nanoparticles synthesized by this approach have an extensive application prospects and can be preserved for a long time.

Acknowledgments

References:

1. Sobczak-Kupiec, A.; Malina, D.; Wzorek, Z.; Zimowska, M. *Micro and Nano Letters.* 2011, 6, 656-660

2. Solanki, J. N.; Murthy, Z.V. P. *Colloid and Surfaces A: Physicochemical Engineering Aspects. 2010,* 359, 31-38

3. Ramaswamy, V.; Vimalathithan, R.M.; Ponnusamy, V. *Advances in Applied Science Research.* 2010,1, 197

4. Song, K. C.; Lee, S. M.; Park, T. S.; Lee, B. S. *Korean Journal of Chemical Engineering.* 2009, 26, 153-155

5. Goia, D.V.; Matijevic, E.; *New Journal of Chemistry.*1998, 98, 1203-1215

6. Zhang, W.; Qiao, X.; Qiu, X. *Journal of Materials Science.* 2009, 44, 1076-1081

7. Rai, M.; Yadav, A.; gade, A. *Biotechnology Advances.* 2009, 27, 76-83

8. Nourafkan, E.; Alamdari, A. *Journal of Industrial and Engineering Chemistry.* 2014, 20, 3639–3645

9. Khadzhiev, Salambek N.; Kadiev, Khusain M.; Yampolskaya, Galina P.; Kadieva, Malkan Kh. *Advances in Colloid and Interface Science.* 2013, 197–198, 132–145

10. McClements, DJ.; Li, Y. *Advances in Colloid and Interface Science.* 2010, 159, 213-228

11. Bilbao Sainz, C.; Avena Bustillos, RJ.; Wood, DF.; Williams, TG.; Mchugh, TH. *Journal of Agricultural and Food Chemistry.* 2010, 58, 11932-11938

12. Jahanzad, F.; Josephides, D.; Mansourian, A.; Sajjadi, S. *Industrial and Engineering Chemistry Research.*2010, 49, 7631-7637

13. Khan, Z.; Al-Thabaiti, S. A.; Obaid, A. Y.; Al-Youbi,A. O. *Colloids and Surface B: Biointerfaces.*2011, 82, 513-517

14. Shukla, P.; Singh, R. P.; Nandi, T. *Oriental Journal of Chemistry.* 2016, 32, 2947-2955

15. Katiyar, A.; Singh, A. N.; Shukla, P.; Nandi, T. *Powder Technology.* 2012, 224, 86-89

16. Bruzzoniti, M. C.; Kobylinska, D. K.; Franko, M.; Sarzanini, C. *Analytica Chimica Acta.* 2010, 665, 69-73

17. Zhang, W.; Qiao, X.; Chen, J.; Wang,H. *Journal of Colloid and Interface Science.* 2006, 302, 370-373

18. de Dios, M.; Barroso, F.; Tojo, C.; Blanco, M. C.; Lopez-Quintela, M. A. *Colloid and Surfaces A: Physicochemical Engineering Aspects.*2005, 270-271, 83-87

19. Capek, I. *Advances in Colloid and Interface Science.* 2004, 10, 49-74

20. Tojo, C.; de Dios, M.; Barroso, F. *Materials.* 2011, 4, 55-72

21. Ee, SL.; Duan, X.; Liew, J.; Nguyen, QD. *Chemical Engineering Journal.* 2008, 140, 626-631

Synthesis and Characterization of Ricinoleic Acid-based Cyclic Carbonates

Padmaja V. Korlipara,* Naganna Narra and Venkateshwarlu Kontham

Centre for Lipid Research,

CSIR- Indian Institute of Chemical Technology, Hyderabad

* *To whom correspondence should be addressed*

Corresponding author E-mail : kvpadmaja@iict.res.in

ABSTRACT

Cyclic carbonates were synthesised from ricinoleic acid by intra molecular rearrangement of epoxy carbonate esters with Lewis acid. The first step was di/mono esterification of ricinoleic acid with 1,4-butane diol, and next step was carbonate interchange reaction between diester/monoester of ricinoleic acid and dimethyl carbonate followed by epoxidation using performic acid method to get epoxy linear carbonates such as **3a** and **3b.** These products on treatment with Lewis acid formed a di/mono cyclic carbonates by intramolecular rearrangement. Synthesized compounds were characterized by ^{1}H NMR, ^{13}C NMR, ESI-MS and FT-IR. In the present study, we report synthesis of new cyclic carbonates from ricinoleic acid. This can be used as monomers for various polymer syntheses such as non-isocyanate polyurethanes (NIPUs).

INTRODUCTION

Vegetable oils are promising renewable resources for polymers. The wide availability of vegetable oils in low prices is considered to be an alternative to the non-renewable petroleum based raw materials and versatile applications (Biermann et al., 2011; Ying et al., 2012). Oleochemical carbonates represent value-added materials derived from renewable resources. These cyclic carbonates have physical and chemical properties which make them useful in personal care, lubricant, fuel additive, and chemical feedstock industries (Kenar et al., 2005). They can be reacted with amines, alcohols, or thiols to form polyurethanes and polycarbonates of varying physical properties(Maisonneuve et al., 2015; Poussard et al., 2016). Cyclic carbonates are generally synthesized by either the reaction of a chlorohydrin, the reaction of a diol with phosgene or, most promisingly, the insertion of carbon dioxide into an epoxide (Doll et al., 2007). Early examples of the phosgene method (Riedeman, 1958; Riedeman,

1958) were used on methyl hydroxy stearates, and the chlorohydrin method has also been shown to produce satisfactory products (Kenar and Tevis, 2005). However, following the principles of green chemistry, avoidance of chlorinated intermediates is preferred.

A more attractive method is carbonated vegetable oils obtained by the reaction of epoxidized vegetable oils with CO_2 using a catalyst. Wilkes and co-workers reported the synthesis of carbonated soybean oil (CSBO) from epoxidized soybean oil (ESBO) using carbon dioxide in 70 h at atmospheric pressure and 110°C, in the presence of tetrabutylammonium bromide as the catalyst with 94% yield. The authors also applied in the preparation of non-isocyanate polyurethane networks by reacting CSBO with different diamines (Tamami et al., 2004). Doll and Erhan enhanced upon this process by using supercritical carbon dioxide and achieved similar conversion of ESO in 20 h (Doll and Erhan 2005; Doll and Erhan 2005).

.

Boyer et al. reported novel linear polyurethanes were synthesized by bulk polyaddition of diamines with two vegetable-based bis-carbonates produced from oleic acid methyl ester (Boyer et al., 2010). Bähr demonstrated that epoxidized vegetable oils were converted into the corresponding cyclocarbonated oils using tetrabutyl ammonium bromide and silica supported alkyl pyridinium iodide in 20 h, to recover catalyst by simple filtration without using any solvents (Bähr and Mülhaupt, 2012). Solvent-free catalytic synthesis of a variety of oleochemical-based cyclic carbonates from CO_2 and the corresponding epoxides by employing various organic halides and polyoxometalates either individually or in combined form was achieved (Langanke et al., 2013). Maisonneuve et al. exhibited the synthesis of more reactive bis 6-membered cyclic carbonates from methyl undecenoate by malonization,

reduction, and carbonation of the resulting diol. The monocyclic carbonate obtained was dimerized either by thiol-ene or the metathesis reaction. Preparation for thermoplastic isocyanate free PHUs from combination of bifunctional 6-membered cyclic carbonates with dodecane-1, 12-diamine (Maisonneuve et al., 2014). Recently, carbonated fatty acid methyl esters were synthesized from epoxy fatty acid esters have been conducted using CO_2, halide salts and phase transfer catalysts and high yields were achieved (Schäffner et al., 2014). In another study bio-based cyclic carbonates were synthesized by coupling CO_2 with epoxidized linseed oil using organo catalysts in combination with hydrogen bond donors (Alves et al., 2015). Castor oil is unique because it contains approximately 85-90 wt% of triglycerides of ricinoleic acid. The presence of hydroxyl and carboxyl groups, as well as C9-C10 unsaturation functional groups make it a potential precursor for the synthesis of many industrial materials. In the present work, ricinoleic acid monoester (RAmE) and ricinoleic acid diester (RAdE, prepared with 1,4-butanediol) were functionalized with dimethyl carbonate reaction to form linear carbonates. In the following reaction, the 9, 10-double bond is converted into epoxide. This epoxide is reacted with Lewis acid to obtain a di and mono cyclic carbonates (Scheme1 and Scheme2). The objective of this work is to synthesize bio-based di/mono cyclic carbonates from castor oil. These carbonates can be potential precursors for the synthesis of isocyanate-free linear polyurethanes, the most promising substitutes for conventional polyurethanes used in paints, coatings and/or as biomaterials.

MATERIALS AND METHODS
Materials

Castor oil was procured from M/s Ramcharan Industries Pvt. Ltd., Hyderabad. Dimethyl carbonate (DMC, 99%), (N, N-dimethylamino)pyridine(DMAP), and scandium (III) trifluoromethanesulfonate ($Sc(OTf)_3$) were purchased from Alfa Aesar (Hyderabad, India). N-(3-Dimethylaminopropyl)-N′-ethylcarbodiimide hydrochloride (EDC·HCl 98%), potassium carbonate anhydrous (K_2CO_3), sodium sulphate (Na_2SO_4), hydrogen peroxide (H_2O_2), and formic acid (HCOOH) were purchased from M/s SD Fine Chemicals (Mumbai, India). Silica gel (60-120 mesh) for column chromatography was purchased from M/s Acme synthetic chemicals (Mumbai, India) and pre-coated TLC plates (silica gel 60 F254) were purchased from M/s Merck (Darmstadt, Germany). Hexane, methanol, dichloro methane (DCM), and ethyl acetate were purchased from Industrial Solvents and Chemicals Pvt. Ltd., (Mumbai, India). All other solvents and reagents were of analytical grade and used directly without purification.

Characterization methods

^{1}H, ^{13}CNMR spectra were recorded on Bruker Avance 700/500 MHz and 175/125 MHz . The NMR spectra were referenced to δ 7.26 ppm and δ 77.0 ppm in $CDCl_3$ solvent for ^{1}H and ^{13}C, respectively. J-coupling pattern in ^{1}H NMR spectra are described as: s = singlet, d = doublet, t = triplet, q = quartet, m = multiplet protons. Mass spectra were recorded using electron spray ionization on Waters e2695 Separators module (Waters, Milford, MA, USA) Mass Spectrometer. FT-IR spectra were recorded in chloroform on a Perkin-Elmer Fourier Transform (FT-IR) Spectrum BX instrument (Model: Spectrum BX; Connecticut, USA). HRMS spectra were obtained by Exactive Orbitrap mass spectrometer (Thermo Scientific, Waltham, MA, USA).

EXPERIMENTAL SECTION

Synthesis of RAdE (ricinoleic acid diester)1a: Under a dry nitrogen atmosphere, ricinoleic acid (6g, 0.020mol) was dissolved in dichloromethane (50 mL), stirred at 0-5 °C. EDC·HCl (4.58g, 0.024mol) were added and stirred for 10 min. 1, 4-butanediol (0.96g 0.010mol) and DMAP (1.2g, 0.01mol) were added and the contents were stirred at 0-5 °C for 10 min. After complete addition, the reaction mixture was stirred at room temperature for 12 h and the progress of reaction was monitored with TLC. After completion of the reaction, the reaction mixture was extracted with dichloromethane, washed with water and dried over anhydrous sodium sulphate and concentrated to

obtain the crude product. The crude product was purified by column chromatography (hexane/ethyl acetate: 92/8 v/v) to obtain **1a** in 80% yield. Similar procedure was followed for the preparation of RAmE (**1b**).

^{1}H NMR (CDCl$_3$, 500 MHz): δ ppm = 5.56 (m, -C$\underline{H}$=CH-), 5.40 (m, -CH=C$\underline{H}$-), 4.12 (t, -C(O)OC$\underline{H}_2$-CH$_2$-), 3.62 (m, -C$\underline{H}$-OH), 2.30 (t, HO-CH-C$\underline{H}_2$-CH=CH-), 2.21 (t, -CH$_2$-C$\underline{H}_2$-C(O)O-), 2.02 (m, -CH=CH-C$\underline{H}_2$-CH$_2$-), 1.62-1.31(multiple signals), 0.88 (t, -CH$_2$-C$\underline{H}_3$). ^{13}C NMR (CDCl$_3$, 125 MHz): δ ppm = 173.97 (-$\underline{C}$(O)OCH$_2$-), 133.30 (-$\underline{C}$H=CH-), 125.26 (-CH=$\underline{C}$H-), 71.27 (-$\underline{C}$H-OH), 63.66 (-C(O)O$\underline{C}$H$_2$-CH$_2$-), 36.74 (HO-CH-C$\underline{H}_2$-CH=CH-), 22.52-35.42 (multiple signals), 14.02 (end carbon of fatty chain). FT-IR: (neat, cm^{-1}) 3447, 2927, 2855, 1737, 1467, 1245, 1174, 725. ESI-MS: m/z 673[M+Na]$^{+}$.

*Synthesis of RAmE (ricinoleic acid monoester)**1b**:* Under a dry nitrogen atmosphere, ricinoleic acid (6g, 0.020 mol) was dissolved in dichloromethane (50 mL), stirred at 0-5 °C, EDC·HCl (4.58g, 0.024mol) was added and stirred for 10 min. Then, 1, 4-butanediol (3.62 g, 0.040 mol) and DMAP (1.2 g, 0.01mol) were added and the contents were stirred at 0-5 °C for 10 min. After complete addition, the reaction mixture was stirred at room temperature for 12 h and the progress of reaction was monitored with TLC. After completion of the reaction, the reaction mixture was extracted with dichloromethane, washed with water and dried over anhydrous sodium sulphate and concentrated to obtain the crude product. The crude product was purified by column chromatography (hexane/ethyl acetate: 90/10 v/v) to obtain **1b** in 90% yield.

^{1}H NMR (CDCl$_3$, 500 MHz): δ ppm = 5.51 (m, -C$\underline{H}$=CH-), 5.41 (m, -CH=C$\underline{H}$-), 4.12 (t, -C(O)OC$\underline{H}_2$-CH$_2$-), 3.68 (t, -CH$_2$-C$\underline{H}_2$-OH), 3.62 (m, -C$\underline{H}$-OH), 2.29 (t, HO-CH-C$\underline{H}_2$-CH=CH-), 2.21 (t, -CH$_2$-C$\underline{H}_2$-C(O)O-), 2.05 (m, -CH=CH-C$\underline{H}_2$-CH$_2$-), 1.62-1.31(multiple signals), 0.88 (t, -CH$_2$-C$\underline{H}_3$). ^{13}C NMR (CDCl$_3$, 125 MHz): δ ppm = 173.97 (-$\underline{C}$(O)OCH$_2$-), 133.30 (-$\underline{C}$H=CH-), 125.26 (-CH=$\underline{C}$H-), 71.27 (-$\underline{C}$H-OH), 63.66 (-C(O)O$\underline{C}$H$_2$-CH$_2$-), 36.74 (HO-CH-C$\underline{H}_2$-CH=CH-), 22.52-35.42 (multiple signals), 14.02 (end carbon of fatty chain).

FT-IR: (neat, cm^{-1}) 3448, 2927, 2855, 1737, 1467, 1245, 1174, 725. ESI-MS: m/z 393 [M+Na]$^{+}$.

Synthesis of 2a: RAdE (6 g, 0.009 mol) was added to K$_2$CO$_3$ (3.8 g, 0.027mol) and DMC (66.4g, 0.738mol) and stirred at reflux temperature of DMC for 35 h. The progress of the reaction was monitored by TLC using hexane/ethyl acetate (90/10 v/v). The reaction mixture was filtered to remove K$_2$CO$_3$ and the filtrate was concentrated under vacuum to remove excess DMC and methanol. The crude product was purified by silica gel column chromatography using hexane/ethyl acetate (98/2 v/v) to obtain **2a** in 88% yield. The product was characterized by ^{1}H NMR, ^{13}C NMR, ESI-MS, and FT-IR spectral analysis. Similar procedure was followed for the preparation of **2b** in 89% yield.

^{1}H NMR (CDCl$_3$, 500 MHz): δ ppm = 5.49 (m, -C$\underline{H}$=CH-), 5.37 (m, , -CH=C$\underline{H}$-), 4.70 (m, -C$\underline{H}$-C(O)OCH$_3$), 4.09 (t-C(O)OC$\underline{H}_2$-CH$_2$-) 3.77 (s, -C(O)OC$\underline{H}_3$), 2.36 (m, -COCH-C$\underline{H}_2$-CH=CH-), 2.30 (t, -CH$_2$-C$\underline{H}_2$-C(O)OCH$_2$-), 2.02 (m, -CH=CH-C$\underline{H}_2$-CH$_2$-), 1.62 (m, -CH$_2$-C$\underline{H}_2$-CH$_2$-), 1.31-1.24 (multiple signals), 0.88 (t, -CH$_2$-C$\underline{H}_3$). ^{13}C NMR (CDCl$_3$, 125 MHz): δ ppm = 174.02 (-$\underline{C}$(O)OCH$_2$-), 155.55 (-O$\underline{C}$(O)OCH$_3$), 133.02 (-$\underline{C}$H=CH-), 123.52 (-CH=$\underline{C}$H-), 78.31 (-$\underline{C}$H-OC(O)OCH$_3$), 63.90 (-C(O)O$\underline{C}$H$_2$-CH$_2$-), 54.75 (-OC(O)O$\underline{C}$H$_3$), 34.52 (-OC(O)-CH-C$\underline{H}_2$-CH=CH-), 22.52-33.11 (multiple signals), 14.11 (end carbon of fatty chain). FT-IR: (neat, cm^{-1}) 3009, 2928, 2856, 1743, 1267, 1173, 791. ESI-MS: m/z 789[M+Na]$^{+}$.

Synthesis of 2b: ^{1}H NMR (CDCl$_3$, 500 MHz): δ ppm = 5.49 (m, -C$\underline{H}$=CH-), 5.37 (m, , -CH=C$\underline{H}$-), 4.69 (m, -C$\underline{H}$-C(O)OCH$_3$), 4.17 (t -CH$_2$-C$\underline{H}_2$OC(O)OCH$_3$), 4.09 (t -C(O)OC$\underline{H}_2$-CH$_2$-), 3.78 (s, -OC(O)OC$\underline{H}_3$), 3.76 (s, -C(O)OC$\underline{H}_3$), 2.36 (m, -COCH-C$\underline{H}_2$-CH=CH-), 2.30 (t, -CH$_2$-C$\underline{H}_2$-C(O)OCH$_2$-), 2.02 (m, -CH=CH-C$\underline{H}_2$-CH$_2$-), 1.62 (m, -CH$_2$-C$\underline{H}_2$-CH$_2$-), 1.31-1.24 (multiple signals), 0.88 (t, -CH$_2$-C$\underline{H}_3$). ^{13}C NMR (CDCl$_3$, 125 MHz): δ ppm = 174.02 (-$\underline{C}$(O)OCH$_2$-), 155.60(-CHO$\underline{C}$(O)OCH$_3$), 154.60(-CH$_2$O$\underline{C}$(O)OCH$_3$), 133.00 (-$\underline{C}$H=CH-), 123.67 (-CH=$\underline{C}$H-), 78.55(-$\underline{C}$H-OC(O)OCH$_3$), 67.46 (-CH$_2$-C$\underline{H}_2$OC(O)OCH$_3$), 63.56 (-C(O)OC$\underline{H}_2$-CH$_2$-), 54.68 (-CH$_2$OC(O)O$\underline{C}$H$_3$), 54.49 (-CH-OC(O)O$\underline{C}$H$_3$), 34.27 (-OC(O)-CH-C$\underline{H}_2$-CH=CH-), 22.52-33.11

(multiple signals), 14.01 (end carbon of fatty chain). FT-IR: (neat, cm^{-1}) 3007, 2927, 2856, 1748, 1267, 1176, 797. ESI-MS: m/z 509 [M+Na]$^{+}$.

Synthesis of 3a: A mixture of **2a** (5 g, 0.0065mol) and formic acid (0.9 g, 0.0195mol) were stirred in a three necked round bottomed flask equipped with an overhead stirrer. 50% aqueous hydrogen peroxide (1.77 g, 0.026mol) was slowly added to the contents at 0 °C for a period of 30 min. After addition, contents were stirred at room temperature for a period of 8 h. The progress of the reaction was monitored by TLC using hexane/ethyl acetate (80/20 v/v). The reaction mixture was extracted with ethyl acetate (70 mL) and washed with water at (3 × 70 mL) until it was acid free and dried over anhydrous Na_2SO_4. The epoxidized product was concentrated by removing the solvent and dried under reduced pressure. The crude product was purified by silica gel column chromatography using hexane/ethyl acetate (96/4 v/v) to get **3a** in 90% yield. Similar experimental procedure was followed for the epoxidation of **2b** to **3b** in 90% yield. The formation of the epoxy ring was confirmed by ^{1}H NMR, ^{13}C NMR, ESI-MS and FT-IR.

^{1}H NMR (CDCl$_3$, 500 MHz): δ ppm = 4.89 (m, -C$\underline{H}$-C(O)OCH$_3$), 4.09 (t -C(O)OC$\underline{H}_2$-CH$_2$-)3.79 (s, -OC$\underline{H}_3$), 3.01 (m, -C$\underline{H}$OCH-), 2.90 (m, -CHOC$\underline{H}$-), 2.30 (t, -CH$_2$-C$\underline{H}_2$-C(O)OCH$_3$), 1.83 (m, -C$\underline{H}_2$-CHOCH-) 1.79 (m, -CHOCH-C$\underline{H}_2$-CH$_2$-), 1.46 (m, -CH$_2$-C$\underline{H}_2$-CH$_2$-), 1.32-1.29 (multiple signals), 0.89 (t, -CH$_2$-C$\underline{H}_3$). ^{13}C NMR (CDCl$_3$, 125 MHz): δ ppm = 173.79 (-$\underline{C}$(O)OCH$_2$-), 155.58 (-O$\underline{C}$(O)OCH$_3$), 77.04 (-$\underline{C}$H-OC(O)OCH$_3$), 63.80 (-C(O)OC$\underline{H}_2$-CH$_2$-), 56.98 (-$\underline{C}$HOCH-), 53.12 (-CHOC$\underline{H}$-), 54.86 (-OC(O)OC$\underline{H}_3$), 34.35 (-$\underline{C}$H$_2$C(O)CH$_2$-), 22.47-33.83 (multiple signals), 14.00 (end carbon of fatty chain). FT-IR: (neat, cm^{-1}) 2927, 2855, 1743, 1444, 1269, 1171, 841, 791. ESI-MS: m/z 821[M+Na]$^{+}$.

Synthesis of 3b: ^{1}H NMR (CDCl$_3$, 500 MHz): δ ppm = 4.88 (m, -C$\underline{H}$-C(O)OCH$_3$), 4.17 (t -CH$_2$-C$\underline{H}_2$OC(O)OCH$_3$), 4.10 (t -C(O)OC$\underline{H}_2$-CH$_2$-), 3.79 (s, -OC(O)OCH$_3$), 3.76 (s, -C(O)OC$\underline{H}_3$), 3.02 (m, -C$\underline{H}$OCH-), 2.91 (m, -CHOC$\underline{H}$-), 2.29 (t, -CH$_2$-C$\underline{H}_2$-C(O)OCH$_3$), 1.80 (m, -C$\underline{H}_2$-CHOCH-) 1.77 (m, -CHOCH-C$\underline{H}_2$-CH$_2$-), 1.46 (m, -CH$_2$-C$\underline{H}_2$-CH$_2$-),

1.32-1.29 (multiple signals), 0.89 (t, -CH$_2$-C$\underline{H}_3$). ^{13}C NMR (CDCl$_3$, 125 MHz): δ ppm =173.69 (-$\underline{C}$(O)OCH$_2$-), 155.67 (-CHO$\underline{C}$(O)OCH$_3$), 155.47(-CH$_2$O$\underline{C}$(O)OCH$_3$), 76.80 (-$\underline{C}$H-OC(O)OCH$_3$), 67.41 (-CH$_2$-C$\underline{H}_2$OC(O)OCH$_3$), 63.54 (-C(O)OC$\underline{H}_2$-CH$_2$-), 56.87 (-$\underline{C}$HOCH-), 53.12 (-CHOC$\underline{H}$-), 54.61 (-CH$_2$OC(O)O$\underline{C}$H$_3$), 54.56 (-CH-OC(O)O$\underline{C}$H$_3$), 34.16 (-$\underline{C}$H$_2$C(O)CH$_2$-), 22.45-33.81 (multiple signals), 13.93 (end carbon of fatty chain). FT-IR: (neat, cm^{-1}) 2923, 2852, 1747, 1443, 1266, 1172, 842, 793. ESI-MS: m/z 525[M+Na]$^{+}$.

Synthesis of di/mono cyclic carbonates: **3a** (3g, 0.0037 mol) was dissolved in DCM (20 mL) and Sc(OTf)$_3$ (0.9g, 0.0018mol) was added and the mixture was stirred at room temperature for a period of 1 h. The progress of the reaction was monitored by TLC using hexane/ethyl acetate (70/30 v/v). The reaction mixture was dissolved in DCM (40 mL) and washed with water at (3×70mL) three times and dried over anhydrous Na_2SO_4. The cyclic carbonate product was concentrated by removing the solvent and dried under reduced pressure. The crude product was purified by silica gel column chromatography using hexane/ethyl acetate (94/6 v/v) to get a dicyclic carbonates 87% yield. Similar procedure was followed for the preparation of monocyclic carbonates. The formation of cyclic carbonate group was confirmed by ^{1}H NMR, ^{13}C NMR, ESI-MS, GC–MS (EI), HRMS, GC and FT-IR.

^{1}H NMR (CDCl$_3$, 500 MHz): δ ppm = 4.55-4.30 (cyclic carbonate ring protons), 3.86-3.77 (m, 1H -C$\underline{H}$-OH), 2.30 (t, -CH$_2$-C$\underline{H}_2$-C(O)OCH$_2$-), 1.30-1.93 (multiple signals) 0.88 (t, -CH$_2$-C$\underline{H}_3$). ^{13}C NMR (CDCl$_3$, 125 MHz): δ ppm = 173.83 (-$\underline{C}$(O)OCH$_2$-), 154.68 and 154.63 (cyclic carbonyl carbon), 82.46-79.49 (cyclic ring carbons), 68.09-67.84 (-CH-OH), 63.75 (-C(O)OC$\underline{H}_2$-CH$_2$-), 34.71 (-$\underline{C}$H$_2$-C(O)OCH$_2$-), 41.29-24.46 (multiple signals) 22.54 (cyclic ring middle carbon), 14.00 (end carbon of fatty chain). FT-IR: (neat, cm^{-1}) 3497 (hydroxy), 2929, 2857, 1801(cyclic carbonate), 1742, 1461, 1438 1174, 1053, 774. ESI-MS: m/z 793[M+Na]$^{+}$. HRMS: calc d for C$_{42}$H$_{75}$O$_{12}$, [M + H]$^{+}$, m/z 771.52512; found, m/z 771.52530.

^{1}H NMR (CDCl$_3$, 500 MHz): δ ppm = 4.52-4.23

(cyclic carbonate ring protons), 4.18 (t -CH$_2$-C$\underline{H}_2$OC(O)OCH$_3$), 4.09 (t -C(O)OC$\underline{H}_2$-CH$_2$-) 3.84-3.76 (m, 1H -C$\underline{H}$-OH), 3.79 (s, -CH$_2$OC(O)OC$\underline{H}_3$), 2.30 (t, -CH$_2$-C$\underline{H}_2$-C(O)OCH2-), 1.30-1.93 (multiple signals) 0.88 (t, -CH$_2$-C$\underline{H}_3$). ^{13}C NMR (CDCl$_3$, 125 MHz): δ ppm = 174.84(-$\underline{C}$(O)OCH$_2$-), 154.61 and 154.56 (cyclic carbonyl carbon), 82.43-79.79(cyclic ring carbons), 68.21-67.95(-CH-OH), 67.41 (-CH$_2$-C$\underline{H}_2$OC(O)OCH$_3$), 63.54 (-C(O)O$\underline{C}$H$_2$-CH$_2$-), 51.43 (-O$\underline{C}$H$_3$),34.72 (-$\underline{C}$H$_2$-C(O)OCH$_2$-), 41.29-24.46 (multiple signals) 22.54 (cyclic ring middle carbon), 14.00 (end carbon of fatty chain). FT-IR: (neat, cm^{-1}) 3509 (hydroxy), 2930, 2857, 1802(cyclic carbonate), 1735, 1463, 1377, 1267, 1176, 1052, 756. ESI-MS: m/z 511[M+Na]$^{+}$.

RESULTS AND DISCUSSION

Ricinoleic acid is obtained from castor oil through hydrolysis, carried out under basic conditions. The first step was di/mono esterification of ricinoleic acid with 1,4-butanediol by using coupling agent EDC·HCl in the presence of DMAP in dichloromethane as solvent to form RAdE and RAmE (**2a** and **2b**) (Venkata Rambabu et al., 2011). Linear carbonates of RAmE and RAdE (**2a** and **2b**) were prepared by dimethyl carbonate interchange reaction between RAmE and RAdE and dimethyl carbonate catalyzed by K$_2$CO$_3$ without any solvent in 87% yields. Different catalysts were reported for dialkyl carbonate interchange reaction (Poussard et al., 2016; Mutlu et al., 2012; Takagaki et al., 2010). However, we have selected K$_2$CO$_3$ due to its effectiveness as a catalyst in synthesizing linear alkyl carbonates and the same was also reported by Rokicki (Tomczyk et al., 2012). The structure of the compounds **2a** and **2b** were confirmed by FT-IR and ^{1}H, ^{13}C NMR spectroscopy. The FT-IR spectra of linear carbonates showed a band at 1742 cm^{-1} for -OC(O)O-, which was overlapped with the carbonyl ester function band. The absence of hydroxyl group band at 3448 cm^{-1} indicated complete conversion of hydroxyl to carbonate groups (Figure 1).
Formation of linear carbonates was also confirmed from their ^{1}H NMR spectra. The methyl proton shift from 3.6 to 4.7 ppm confirmed the formation of

carbonate moiety in **2a** and **2b** (Figure 2). A singlet at 3.6 ppm for new methoxy protons (-OCH$_3$) for **2a** and **2b** in ^{1}H NMR spectra confirmed the linear carbonate structure (Figure 2). Multiplets at 5.3-5.5 ppm indicated 9, 10-double bond protons in both the compounds. The remaining protons for alkyl chain well matched in ^{1}H NMR spectra. In ^{13}C NMR spectra, the carbonate carbon appeared at 155 ppm whereas ester carbon appeared at 173 ppm (Figure 3). This is due to the electron releasing effect of the additional oxygen atom compensating for electron withdrawal of the carbonyl oxygen (Kenar et al., 2004). The appearance of chemical shift at 76 ppm confirmed the complete conversion of hydroxyl to carbonate group. The olefinic carbons appeared at 133 ppm and 126 ppm indicating the presence of double bond. The epoxidation of double bond in **2a** and **2b** was carried out using the modified performic acid method to obtain **3a** and **3b** (Doll et al., 2013; Sharma et al., 2007; Findley et al., 1945; Schmitz et al., 1954). The structure of epoxy products **3a** and **3b** was confirmed by FT-IR and ^{1}H NMR, ^{13}C NMR studies. The formation of the epoxy group was observed in the FT-IR spectra at 841 cm^{-1} (Figure 1) and also observed disappearance of double bond band at 3007 cm^{-1} confirmed complete conversion of unsaturation into epoxy group. The protons on the epoxy group carbons appeared at 2.8-2.9 ppm for **3a** (Figure 2) and at 2.9-3.0 ppm for **3b** in ^{1}H NMR spectra confirmed the presence of epoxy group. New peaks were observed in ^{13}C NMR spectra of epoxy carbons at 53-56 ppm in both the products (Figure 3). The mass spectrum of **3a** and **3b** at m/z 821[M+Na]$^{+}$ and 525 [M+Na]$^{+}$ for both the compounds (Figure S$_3$ and S$_8$, Supporting Information).
The epoxy carbonate esters (**3a** and **3b**) were treated with Lewis acid such as Sc(OTf)$_3$ gave a di/mono ester of mixture of inseparable five and six membered cyclic carbonates (Naganna et al., 2016). The cyclic carbonates were characterized by ^{1}H NMR, ^{13}C NMR, ESI-MS, HRMS and FT-IR.
The chemical structures of the cyclic carbonates were also confirmed by NMR analyses, as illustrated in Figure 2 and Table 1 for five and six membered cyclic carbonate di/mono esters. The disappearance of proton NMR signals at 2.8, 3.02,

and 3.63 ppm corresponding to epoxy protons and methoxy carbonated protons and appearance of new proton NMR signals at 4.52, 4.26 (cyclic ring protons) and 3.77 ppm (CH-OH) confirmed the cyclic carbonate structure (Figure 2). The ^{13}C NMR spectroscopic data also revealed that the cyclic carbonate ester mixture contained both five and six membered rings. ^{13}C NMR spectrum (Figure 3) showed the presence of two carbonyl carbon atoms in adjacent position at 154.23, 154.41 ppm and two carbonate rings carbon signals in at 82.43, 82.02 ppm and 79.81, 79.47 ppm. This proved the presence of the two cyclic carbonates rings in the product mixture. The NMR values are well in agreement with the reported values for five membered fatty acid-based cyclic carbonate compounds [9-14]. The other carbon chain values were in the range of 41.34-14.00 ppm. The cyclic carbonates formation was also confirmed from their mass spectral analysis, showing m/z 793 $[M+H]^+$ and molecular formula of $C_{42}H_{75}O_{12}$ obtained from HRMS (Figure S_5 Supporting Information). FT-IR spectroscopy showed the presence of two bands at 1801 and 774 cm^{-1} corresponding to the cyclic carbonyl functions of cyclic carbonates respectively. This also matched well with the reported data [9-14]. Besides this, a large band appeared at 3497 cm^{-1} which is attributed to the OH vibrations (Figure 1).

Table 1: NMR values of cyclic carbonates

Functional groups	^{1}H-NMR	^{13}C-NMR
Monocyclic carbonates of terminal -OCH$_3$ group	3.79ppm	51.43ppm
Cyclic carbonate ring	4.55-4.30ppm(cyclic ring protons)	82.43-79.79ppm(cyclic ring carbons)

CONCLUSIONS

In this article, we report synthesis of ricinoleic acid based cyclic carbonates following a three-step procedure for the first time. The first stage was esterification then next interchange reaction followed by epoxidation and finally Lewis acid catalyzed rearrangement. The prepared carbonates can be potential precursors for biodegradable polymeric materials (Maisonneuve et al., 2014).

Correspondence: Dr. K V Padmaja, Centre for Lipid Research, CSIR-Indian Institute of Chemical Technology, Uppal Road, Hyderabad 500007, India.
E-mail: padmajak@iict.res.in
Fax: +91-40-27193370.

REFERENCES

Alves, M., Grignard, B., Gennen, S., Detrembleur, C., Jerome, C., Tassaing, T., 2015.Organocatalytic synthesis of bio-based cyclic carbonates from CO$_2$ and vegetable oils. **RSC Advances, 5 (66), 53629-53636.**

Bähr,M., Mülhaupt, R., 2012. Linseed and soybean oil-based polyurethanes prepared via the non-isocyanateroute and catalytic carbon dioxide conversion. **Green Chem.14, 483-489.**

Biermann, U.,BornscheuerU., Meier,M. A. R., Metzger,J. O., Schäfer,H. **J. 2011.Oils and fats as renewable raw materials in chemistry Angew Chem. Int. Ed. 50, 3854-3871.**

Boyer, A., Cloutet, E., Tassaing, T., Gadenne, B., Alfos, C., Cramail, H.2010. Solubility in CO$_2$ and carbonation studies of epoxidized fatty acid diesters: Towards novel precursors for polyurethane synthesis. **Green Chem.12, 2205–2213.**

Doll,K. M, Bantchev, G. B., Murray, R. E., 2013. Bismuth (III) Trifluoromethanesulfonate catalyzed

ring-opening reaction of mono epoxy oleochemicals to form keto and diketo derivatives **ACS Sustainable Chem. Eng.1, 39-45.**

Doll, K. M., Erhan, S. Z., 2005.Synthesis of carbonated fatty methyl esters using supercritical carbon dioxide. **J. Agric. Food Chem.53, 9608-9614.**

Doll, K. M., Erhan, S. Z., 2005.The improved synthesis of carbonated soybean oil using supercritical carbon dioxide at a reduced reaction time. **Green Chem.7, 849-854.**

Doll, K. M., Kenar, J. A., Erhan, S. Z., 2007.Carbonates from oleochemicals: biobased materials to value added green chemicals, **Chem. Today. 25, 7-10.**

Findley, T. W., Swern, D., Scanlan, J. T., 1945. Epoxidation of unsaturated fatty materials with peracetic acid in glacial acetic acid solution. **J. Am. Chem. Soc.67, 412-414.**

Kenar, J. A., Knothe, G., Copes, A. L., 2004. Synthesis and characterization of dialkyl carbonates prepared from mid-, long-chain, and guerbet alcohols. **J. Am. Oil Chem. Soc.81, 285-291.**

Kenar, J. A., Knothe, G., Dunn R. O., Ryan, T. W. I., Matheaus, A.,2005. Physical properties of oleochemical carbonates. **J. Am. Oil Chem. Soc. 82, 201-205.**

Kenar,J. A., Tevis,I. D.,2005.Convenient preparation of fatty ester cyclic carbonates. **Eur. J. Lipid Sci. Technol. 107, 135-137.**

Langanke, J.,Greiner, L., Leitner, W., 2013.Substrate dependent synergetic and antagonistic interaction of ammonium halide and polyoxometalate catalysts in the synthesis of cyclic carbonates from oleo chemical epoxides and CO_2. **Green Chem.15, 1173–1182.**

Maisonneuve, L., Lamarzelle, O., Rix, E., Grau, E., Cramai, H., 2015. Isocyanate-free routes to polyurethanes and poly(hydroxy urethane)s. **Chem. Rev. 115, 12407-12439.**

Maisonneuve, L., More, A. S., Foltran, S., Alfos, C., Robert, F., Landais, Y., Tassaing, T., Grau, E., Cramail, H., 2014. Novel green fatty acid-based bis-cyclic carbonates for the synthesis of isocyanate-free poly(hydroxyurethane amide)s. **RSC Adv. 4, 25795-25803.**

Maisonneuve, L., Wirotius, A. L., Alfos, C., Grau, E., Cramail H., 2014. Fatty acid-based (bis) 6-membered cyclic carbonates as efficient isocyanate free poly(hydroxyurethane) precursors. **Polym, Polym. Chem.5, 6142-6147.**

Mutlu, H., Ruiz, J., Solleder, S. C., Meier, M. A. R.,2012. TBD catalysis with dimethyl carbonate: a fruitful and sustainable alliance. **Green Chem. 14, 1728-1735.**

Naganna, N, Prasad, R. B. N., Phanibabu, S. V., Padmaja. K. V., 2016. Lewis-acid catalyzed synthesis and characterization of novel castor fatty acid-based cyclic carbonates. **RSC Adv. 6, 25703-25712.**

Poussard, L., Mariage, J., Grignard, B., Detrembleur, C., Jeró me C., Calberg C., Heinrichs, B., De Winter, J., Gerbaux, P., Raquez, J. M., Bonnaud, L., Dubois, Ph., 2016.Non-isocyanate polyurethanes from carbonated soybean oil using monomeric or oligomericdiamines to achieve thermosets or thermoplastics. **Macromolecules 49, 2162−2171.**

Riedeman,W. I., Carbanato esters of fatty acids. **U.S. Patent 2,826,591, March 11, 1958.**

Riedeman,W. I., Plastic composition containing carbonate esters of fatty acids. **U.S. Patent 2,858,286, Oct 28, 1958.**

Schäffner. B., Blug, M., Kruse, D., Polyakov, M., Köckritz, A., Martin, A., Rajagopalan P., Bentrup, U., Brückner, A., Jung, S., Agar, D., Rüngeler, B., Pfennig, A., Müller, K., Arlt, W., Woldt, B., Grass, M., Buchholz, S., 2014. Synthesis and application of carbonated fatty acid esters from carbon dioxide including a life cycle analysis. **ChemSus Chem. 7, 1133 - 1139.**

Schmitz, W. R., Wallace, J. G., 1954.Epoxidation of methyl oleate with hydrogen peroxide. **J. Amer. Oil Chem. Soc.31, 363-365.**

Sharma, B. K., Doll, K. M., Erhan, S. Z., 2007. Oxidation, friction reducing, and low temperature properties of epoxy fatty acid methyl esters. **Green Chem. 9, 469-474.**

Takagaki, A., Iwatani, K., Nishimura, S., Ebitani,

K., 2010. Synthesis of glycerol carbonate from glycerol and dialkyl carbonates using hydrotalcite as a reusable heterogeneous base catalyst. **Green Chem. 12, 578-581**

Tamami, B., Sohn, S.,Wilkes, G. L, 2004. Incorporation of carbon dioxide into soybean oil and subsequent preparation and studies of nonisocyanate polyurethane networks. **J. Appl. Polym. Sci. 92, 883-891.**

Tomczyk,M., K., Guńka, P. A., Parzuchowski, P. G., Zachara, J., Rokicki, G., 2012. Intramolecular etherification of five-membered cyclic carbonates bearing hydroxyalkyl groups. **Green Chem. 14, 1749-1758. Vz**
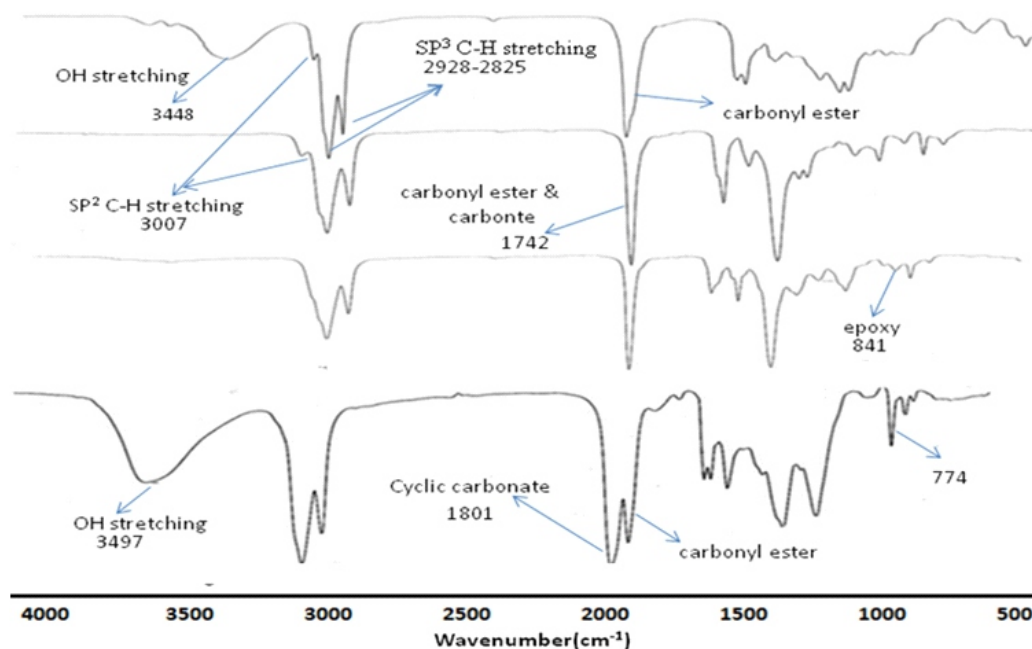
Fig.1: Stacked FT-IR spectra of top to bottom RAdE,2a,3a, di-cyclic carbonates.
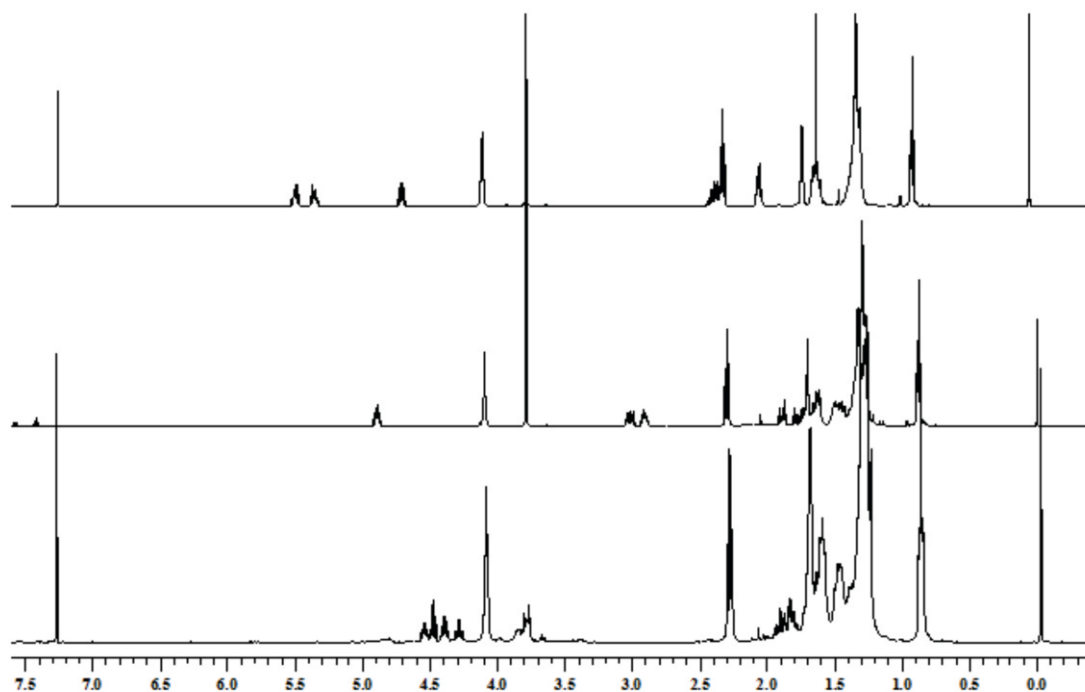
Fig. 2: Stacked ^{1}H NMR spectra of 2a (top),3a (middle), di-cyclic carbonates (bottom).
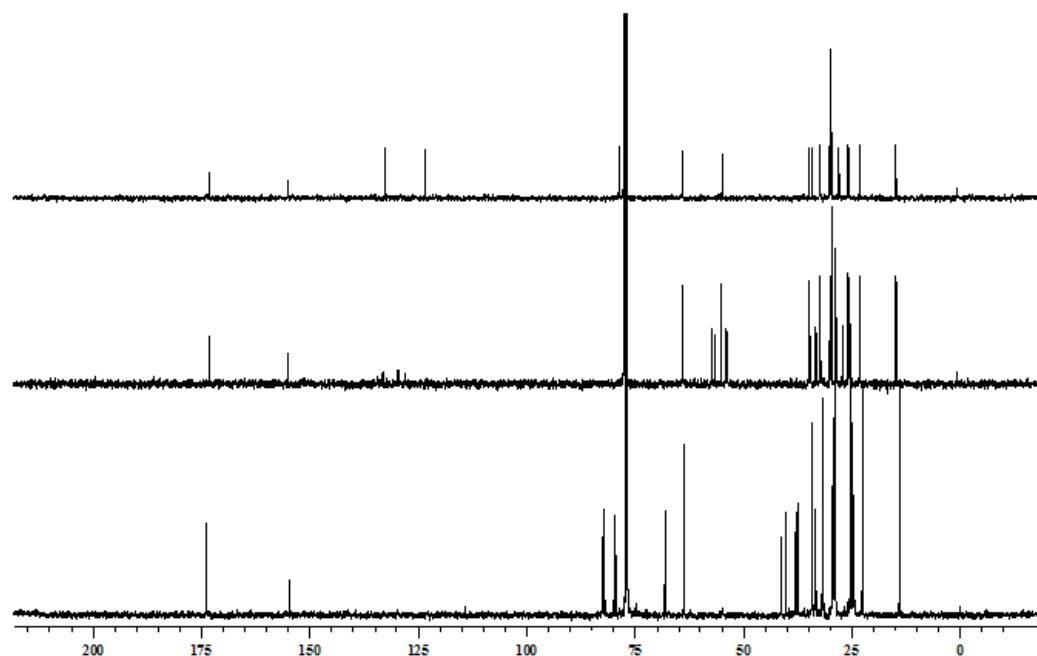
Fig. 3: Stacked ^{13}C NMR spectra of 2a (top),3a (middle), di-cyclic carbonates (bottom).
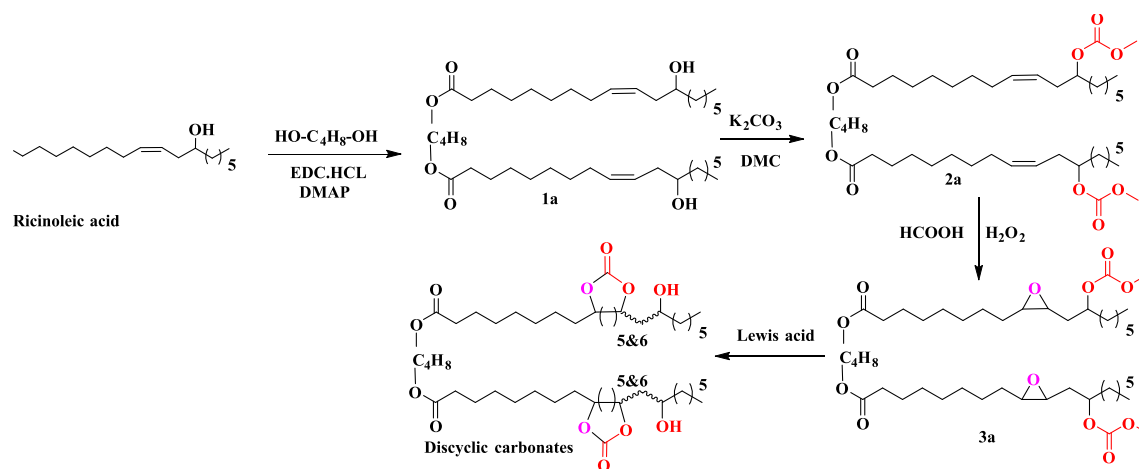
Scheme1. Chemical synthesis of di-cyclic carbonates
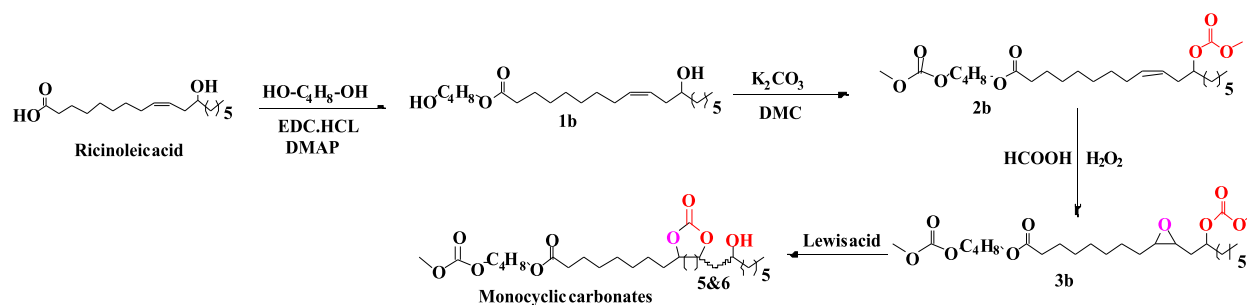
Scheme2. Chemical synthesis of mono cyclic carbonates

Oil expression from *Simarouba glauca* kernels using a manual hydraulic screw press

S. K. Satpathy[a], S. N. Naik[b] and R.Prasad[b]

[a] College of Agricultural Engineering and Post-Harvest Technology, Central Agricultural University, Gangtok, Sikkim, India

[b] Centre for Rural Development & Technology, Indian Institute of Technology, Delhi, India

Corresponding author : S. N. Naik, Email: snn@rdat.iitd.ac.in

Abstract

The objective of the present study was to study the effect of pressure and pressing time on the oil yield of *Simarouba glauca* using a manual hydraulic screw press.The physico-chemical properties of the oil were also studied. The feed samples at dry basis moisture level of 6.54% were cooked at 100°C for 30 min before oil expression. Pressing experiments were conducted at pressures of 20, 25, 30 and 35 MPa and pressing time of 5, 10, 15 and 20 min. The optimum oil recovery was 83.7% (w/w) at a pressure of 30 MPa with 15 min pressing time. The oil expressed under the processing condition investigated is of acceptable quality. The oil recovery percentage in the manual hydraulic press is at par with that of the oil recovery in mechanical screw presses.

1. Introduction

an evergreen tree producing seeds with high oil content (50-65%,w/w) with a potential of producing 2 t oil/ha. Simarouba seed oil is suitable for both edible and non-edible purposes. The use of S. glaucaas a vegetable oil crop was first considered near the end of 1939 in Central America and introduced in India in 1966 (Joshi &Hiremath, 2000). Armour (1959) reported that tests confirmed the suitability of simarouba oil for human consumption in all respect. Monseur&Motte (1983) reported that the seeds of S. glaucaare rich in edible fat (nearly 60 % w/w) that canbe used for cooking.It can also be used to manufacture vanaspati, vegetable butter and margarine. S.glaucahas also been considered for biofuel production (Patil&Gaikwad, 2011). Biodiesel of Simarouba glaucais a simple biodegradable, nontoxic and essentially free from sulphur and aromatics and can be used in compressionignition engines as a blend with petroleum diesel. The oil cake, fruit pulp, leaf litter and unwanted wood can be used to generate biogas. The shell and waste wood can be used in thermal power generation. The lignocellulose contained in the huge amount of biomass produced (about 15 tones/ ha /yr) can be used as feedstock for manufacturing second generation biofuels (Patil&Gaikwad, 2011).

Considering its food and fuel value, large scale plantation has been taken up by the government in Orissa, Karnataka, Andhra Pradesh and other states of India. Presently the oil seeds are collected in rural areas, processed in traditional methods and the crude oil is used for consumption (Rama et. al., 2003, Rout et. al. 2014). Simarouba seeds contain about 70% hull by weight and it is very hard and difficult to crush directly in an expeller (Jena et.al, 2003). Therefore, processing of Simarouba essentially involves decortication and oil extraction.

Oil is extracted from oil seeds by either mechanical or chemical methods. In chemical method oil is extracted using a chemical solvent like hexane. Traces of the solvent in the extracted oil adversely affect the quality of the oil and also pose environmental concerns (Santoso et. al 2014). In mechanical method, oil is expressed by using a batch type hydraulic press or continuous type screw press machines (Khan & Hanna, 1983). Mechanical oil expellers are widely popular in India for extraction of oil from oil bearing seeds. However, limited reported literature is available on simarouba oil extraction by mechanical oil expellers. Jena et. al. (2013) reported that Simarouba glaucabeing a low fibre and high oil bearing seed resulted in the formation of a semi solid paste during oil expression in the continuous screw press and no oil recovery was obtained. Hence, it was desired to use a mixture of 40-50% kernels by weight andpress cake for efficient oil recovery in the screw press.Similar findings were also reported by Armour (1959) that 20-35% (w/w) of simarouba hull or press cake had to be mixed with the kernels for efficient oil recovery in anAnderson duo expeller.In order to overcome these problems, a hydraulic press may be used instead for small scale applications. For small and medium scale applications, the hydraulic press is quite appropriate as it requires lower initial costs (Ajibolaet al., 2000).

In a hydraulic press, the oil seeds are subjected to intense pressure and the oil bearing cells are weakened; they get ruptured and discharge their contents (Oyinlola&Adekoya, 2004; Ajibolaet al., 2002; Hamzat& Clarke, 1993). Oil expression in hydraulic press requires an understanding of the mechanical behaviours of oil seeds under compressive load.

The compressive load, pressing/holding time, seed moisture content, seed conditioning or cooking affects oil yield in rapeseeds, sunflower seeds, jatropha seeds, soybean etc. (Herak et. al, 2012; Mwithigaand Moriasi, 2007; Sukumaran and Singh, 1989). Knowledge of the pressure that will optimize oil recovery from a particular oil seed is therefore very important for the process to be efficient (Ogunsina, 2014). No study on this aspect hasso far been reported for simarouba seeds.

In view of the above, this study was undertaken to investigate the effect of pressure and pressing time onyield from conditioned Simarouba oil seed kernels using a custom built manual hydraulic screw press. This information would be helpful in identifying the optimum processing conditions for efficient operation of the hydraulic screw press.

2. Material and Methods

2.1 Raw materials and sample preparation
Simarouba seeds were procured from Koraput (Odisha, India). The seeds weredecorticated using a custom built power operated decorticator. The decorticated kernels were used for oil

extraction. Prior investigation for expression of oil under compressive load were carried out in laboratory using a test cell and Instron UTM for various moisture content of kernels (4.54-8.74 % w/w, db), cooking temperature (70-110°C), cooking time (10-30 min). Optimum oil yield was obtained in kernels of 6.54% dry basis moisture content, cooked at 100°C for 30 min and compressed at a maximum pressure of 24.99 MPa. These optimum moisture content and cooking conditions were used in the present study.

The initial moisture content of simarouba kernel was determined by standard hot-air oven method at 105°C for 24 h (Pradhan et. al. 2008). The initial moisture content of the kernel was 4.54 % dry basis (db). The moisture content of the kernels was adjusted to the optimum moisture content of 6.54%w/w(db) by spraying the calculated amount of water (Pradhan et. al. 2008). These conditioned kernel samples were stored in high-density polyethylene, air tight bags of 100 mm thickness. These bags were kept at 4°C in a refrigerator for a week for uniform moisture distribution. Simarouba kernels were cooked in a hot-air oven (Yorco Sales Pvt. Ltd, India)at the optimized cooking conditions of 100°C for 30 minutes. These cooked kernels were utilized for further investigation. The conditioned and cooked kernels were pressed in a custom

built manual hydraulic screw press.

2.2 Description of the manual hydraulic screw press
The manual hydraulic screw press used in the present study consisted of a mild steel H frame, a press piston with screw, a perforated cylindrical oil cage of internal diameter 130 mm and height of 450 mm, a manual hydraulic jack of 50t capacity, working platform with oil trough and a lead screw handle (Fig. 1). A pressure gauge was fitted with the hydraulic jack to record the applied pressure. The working platform rests on the hydraulic jack placed at the bottom of the frame. The cylindrical oil cage is placed on the working platform. Initially compression of the kernels inside the oil cage was achieved by manual turning of the screw and downward movement of the press piston. The samples were finally subjected to the desired pressure with the help of the hydraulic jack by manual movement of the pump handle. The pressure was released after the desired pressing time. The expressed oil was collected from the outlet channel of the oil trough.

2.3 Oil extraction and analysis
Oil extraction was carried out at different pressures (20, 25, 30, 35 MPa) and pressing times (5, 10, 15, 20 min). A full factorial design with three replications was followed. About 3±0.01 kg of conditioned simarouba kernels were pressed in the hydraulic screw press in each experimental run. After pressing, the crude oil was collected and weighed. Residual oil content in the cake was also determined. Oil recovery percent was estimated for each experimental run using Equation (1) (Pradhan et. al, 2011). The process parameters were optimized for highest oil recovery percent. The oil content in the kernel and cake was determined by direct gravimetric method of solvent extraction using n-hexane (AOAC, 1984). The extracted crude oil at optimum processing conditions was also analysed for some physico-chemical properties viz., density, viscosity, acid value, free fatty acids content,

density, iodine value and saponification value using methods described by the Association of Official Analytical Chemists (AOAC, 1984).

$$\% \; oil \; recovery = \left(1 - \frac{W_c O_c}{W_i O_i} \right) \times 100$$

Where, W_c (kg) is weight of cake, O_c is the percentage of oil content in cake, W_i (kg) is weight of kernel sample, O_i is the percentage oil content in kernel sample.

The fatty acid composition of the oil was determined bygas

chromatograph equipped with a flame ionization detector (Nucon Engineers, Delhi, India), with fused silica capillary column BPX 70. The column temperature was programmed to increase from 180 °C to 240 °C at 4 °C/min. The detector and injector temperature was set at 240 °C and 230 °C respectively. The carrier gas used was nitrogen (40 psi) at a flow rate of 45.0 mL/min and air and hydrogen were used at flow rates 30 mL/min and 300 mL/min respectively. The sample injection volume was 1.0 µL with a split flow of 60 mL/min. The internal standard used was methyl heptadecanoate (Sigma Aldrich, USA).
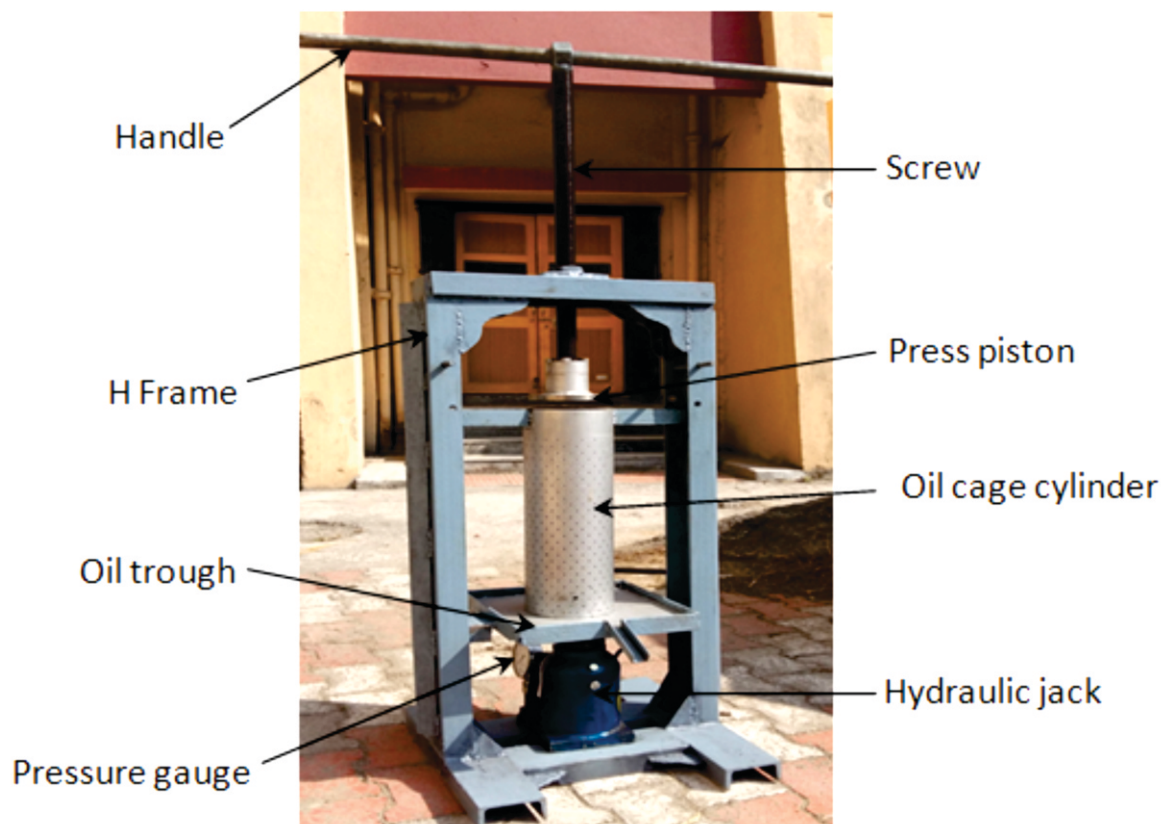
Fig. 1: View of the hydraulic screw press used in the study

2.4. Statistical analysis

The experimental data was analysed using SPSS 16.0 software for windows. ANOVA was carried out to analyse the effects of pressure and pressing time on the oil recovery percent. Duncan's multiple range test (DMRT) was also done to compare significant difference between means.

3. Results and Discussion

3.1. Effect of pressure and pressing time on oil recovery percent

The average oil recovery percent and residual oil in cake obtained at different pressure and pressing time is given in Table 1. From Table 1, it can be observed that the mean oil recovery percent varied between 68.33% (w/w) and 84.59% (w/w) for various experimental conditions. The maximum oil recovery percent of 84.59% was obtained at a pressure of 30Mpa and pressing time of 20 minutes. The corresponding residual oil content in the cake was 17.9% (w/w).Severen (1953) reported expression of simarouba fat in a box hydraulic press operated at a pressure of 34.5 MPa with the kernels cooked at 100°C for 20minutes. The cake contained about 17% (w/w) oil. Oil recoveries of 72-89 % (w/w) were reported for simarouba kernels in a mechanical screw press depending upon the cake content in the feed (20-50 %, w/w) by Jena et. al, 2003. Very low simarouba oil yield of only 15% in mechanical screw press as against 55-60% (w/w) oil yield in solvent extraction has also been reported by Mishra et. al. (2012).

Table 1. Oil recovery percent during hydraulic pressing of simarouba kernels

Pressure, Mpa	Pressing time, min	Mean Oil recovery, %	Residual oil in cake, %
20	5	68.33 (0.59)	30.95(1.20)
	10	70.46 (0.36)	29.48(0.97)
	15	71.71(0.73)	28.60(1.31)
	20	72.19 (0.69)	28.24(0.76)
25	5	71.45 (0.92)	28.78(1.03)
	10	73.34 (1.07)	27.40(0.64)
	15	75.82(1.91)	25.50(0.83)
	20	76.21 (0.44)	25.19(1.34)
30	5	80.15 (1.15)	21.94(0.91)
	10	81.46 (0.64)	20.79(0.77)
	15	83.70(0.49)	18.75(0.42)
	20	84.59 (0.71)	17.90(0.55)
35	5	79.07 (0.50)	22.85(0.61)
	10	80.51 (0.64)	21.62(0.52)
	15	82.43 (1.03)	19.91 (0.66)
	20	83.40 (0.87)	19.02 (1.10)

Values in parentheses indicate standard deviation.

The effect of pressure and pressing time on oil recovery percent is depicted in Fig. 2. The oil recovery percent increased with increase in pressure up to 30MPa at all pressing times. Beyond this pressure, oil yield percent decreased and residual oil content in cake increased. As the pressure is increased, oil flows through the interstices of the kernel mass and moves out. But at pressure above 30 MPa, there may be a sealing effect of these interstices resulting in plastic flow of solid instead of oil flow. This results in decreased oil recovery percent. Similar type of behaviour has been reported by Sivalaet. al. (1993) during oil expression from rice bran using hydraulic press. The oil recovery percent increased with increase in pressing time at all pressures. This implies that the residual oil content in cake decreased with increase in pressing time within the pressure range studied. Similar type of results has been reported for oil expression from rice bran (Sivala et. al. 1993), rubber seeds (Santoso et. al. 2014) and soybean (Mwithiga&Moriasi, 2007) using hydraulic press.

3.2. Statistical analysis of results

The analysis of variance (ANOVA) for the oil recovery percent is shown in Table 2. From Table 2, it can be seen that the effect of both pressure and pressing time on oil recovery percent is significant (p <0.01). The average oil recovery percent significantly increased with increase in pressure and pressing time. However, the interaction effect of pressure and pressing time was found to be non-significant (p > 0.05).
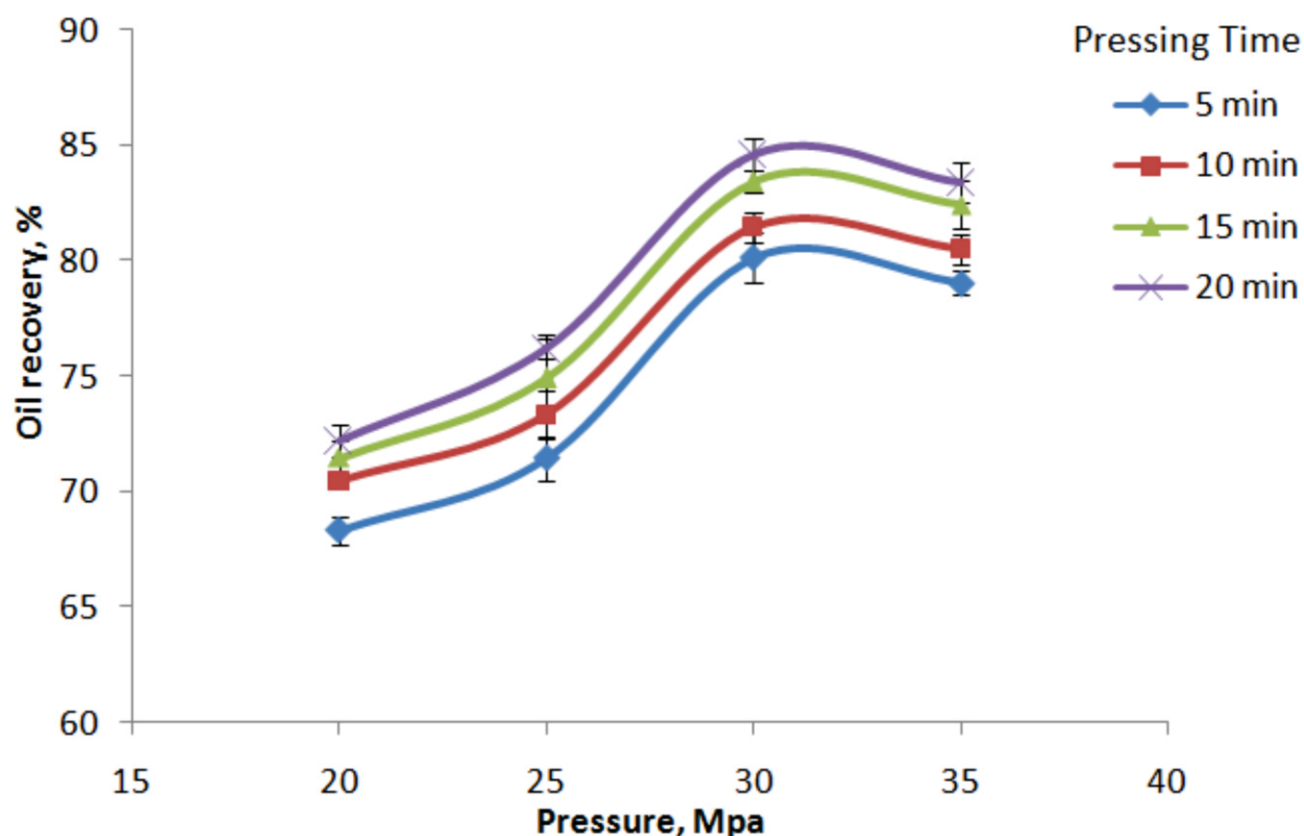
Fig. 2: Effect of pressure and pressing time on oil recovery percent of simarouba   kernels

Table2. Analysis of variance of oil recovery percent showing effect of pressure and pressing time

Source	Sum of Squares	Degree of freedom	Mean Square	F value	Sig.
Intercept	285896.331	1	285896.331	3.631E5	.000
Pressure	1159.859	3	386.620	491.064	.000
Pressing time	139.910	3	46.637	59.235	.000
Pressure * pressing time	2.869	9	.319	.405	.923
Error	25.194	32	.787		
* Significant at p < 0.01					

Table 3 represents the results of post hoc analysis using Duncan's multiple range teststo the means of the effect of pressure and pressing time on oil recovery percent. From the table it can be observed that the mean values of oil recovery percent is significantly different (p<0.05) between all levels of pressure. However, the difference between the mean values of oil recovery percent at pressing time of 15 and 20 minutes was found to be insignificant. Hence, pressing time of 15 minutes may be recommended in view of time saving and increase in press capacity.

Table 3. Effect of pressure and pressing time on oil recovery percent (Post-Hoc Analysis)

Pressure, MPa	Oil recovery, %(w/w)
20	70.67[a]
25	74.20[b]
30	82.47[c]
35	81.35[d]
Pressing Time, Min	
5	74.75[a]
10	76.44[b]
15	78.41[c]
20	79.10[c]

Values in the same columns followed by different alphabets (a–d) are significant ($P < 0.05$).

3.3 Some physico-chemical properties and fatty acid composition of simarouba oil

The importance of physico-chemical properties in determining the quality of simarouba oil cannot be overlooked. The values of the physico-chemical properties of simarouba oil extracted at optimum conditions of pressing were measured and are shown in Table 4 along with literature values for crude simarouba oil.

The acid value of extracted simarouba oil was found to be 4.34, which is well within the range of acid value of 2.25-8.4as reported in literature for crude simarouba oil. Crude vegetable oils usually have high free fatty acid levels (half of acid value) as enzyme lipase are activated by moisture in such cases, which results in hydrolysis initiation and increase in the free fatty acid content (Weiss, 1983). Iodine value indicates the degree of unsaturation of the oil and a high iodine value indicates oil prone to oxidation. The measured iodine value of (53.1± 2.06) in the extracted simarouba oil is in close agreement with the reported literature values. The simarouba oil has lower iodine value than sunflower oil (94.34), corn oil (97.35), rapeseed oil (95.12) and peanut oil (102.02) (Neagu et. al., 2013), whereas it has iodine value close to that of crude palm oil (47-55.83) (Koushki et. al., 2015). Saponification value is a measure of oxidation during storage, and also indicates deterioration of the oils (Neagu et. al., 2013). The measured saponification value (191.7) is within the range of reported literature values and is comparable to that of sunflower oil (192.65) and groundnut oil (193.45) (Preetiet. al., 2007). A high saponification value indicates that oils are normal triglycerides and very suitable in the production of liquid soap and shampoo (Pradhan et. al., 2011). Viscosity and density are the parameters required by biodiesel and diesel fuel standards because of being key fuel properties for diesel engines (Alptekin&Canakci, 2008). The density and viscosity values of crude simarouba oil were 883 kg. m^{-3} and 62.4×10^{-6} m^2.s^{-1} respectively. These values were well within the reported values cited in literature.

Table 4: Physico-chemical properties and fatty acid composition of simarouba oil

Properties	Measured values	Literature values[*]
Acid value	4.34 (0.87)	2.25 – 8.4
Iodine value,	53.1 (2.06)	52.6 - 54.3
Saponification value	191.7 (9.34)	176 – 192.3
Density, $kg.m^{-3}$	886 (135)	860 - 907
Kinematic viscosity (40°C), $m^2.s^{-1}$	62.4×10^{-6} (4.81)	34×10^{-6} - 73.7×10^{-6}
Fatty acid %		
Palmitic acid (C16:0)	11.88	10.9-14.8
Stearic acid (C18:0)	28.46	25.6-27.3
Arachidic acid (C20:0)	0.22	1.2-1.8
Oleic acid (C18:1)	56.12	52.6-59.1
Linoleic acid (C18:2)	1.70	2.3-3.3
Linolenic acid (C18:3)	1.62	0.2-0.35
Total SFAs	40.39	36.5-39.9
Total MUFAs	56.29	52.9-59.1
Total PUFAs	3.32	2.5-3.65

Values in parentheses indicate standard deviation.
* Source: Patil et. al. (2011); Mishra et. al. (2012a, b), Jena et. al. (2010); Duhan et. al. (2011); Rout et. al. (2014)

The major fatty acids found in the extracted simarouba oil were oleic (56.12%), stearic (28.46%) and plamitic acid (11.88%). The fatty acid composition is similar to the reported literature values. It contained saturated fatty acid (SFA) (40.39%), monounsaturated fatty acid (MUFA) (56.29%) and polyunsaturated fatty acid (PUFA) (3.32%). The fatty acid profile of the simarouba oil is similar to palm oil (SFA = 49.9%, MUFA= 39.2% and PUFA = 10.5%) (Mancini et. al., 2015).Duhanet. al. (2011) reported that the oleic acid value in *S. glauca*was found very much comparable with rapeseed oil and indicates its edible utility.

4. Conclusion
The results in the present study revealed that extraction pressure and pressing time have significant effects on the oil recovery percent from simarouba kernels extracted in a manual hydraulic screw press. The optimum pressing conditions are found to be a pressure of 30 MPa and 15 minutes pressing time with an oil recovery of 83.7%. The oil recovery in the manual hydraulic screw press is comparable and in cases higher than that for mechanical screw presses. The physico-chemical properties and fatty acid composition of the extracted simarouba oil is at par with the values reported in literature and indicates its acceptable quality. The simarouba oil resembles palm oil and rapeseed oil with respect to its properties. The manual hydraulic press can efficiently express oil from simarouba kernels and is suitable for small scale applications in rural areas.

REFERENCES

A.O.A.C., 1984,"Official methods of analysis of the Association of Official Analytical Chemists (13th ed.)", Washington DC, Association of Official Analytical Chemists.

Ajibola, O.O., Eniyemo, S. E., Fasina, O. O., and Adeeko, K. A., 1990,"Mechanical expression of oil from melon seeds", **Journal of Agricultural Engineering Research 45, 45-53.**

Alptekin, E., andCanakci, M., 2008,"Determination of the density and the viscosities of bio diesel fuel blends", **Renewable Energy 33, 2623-2630.**

Armour, R.P., 1959,"Investigation on *Simarouba glauca* DC. In EI Salvador", **Economic Botany 13, 41-66.**

Duhan, A., Suthar, Y.,Moudgil, H., andDuhan, S., 2014, "Effect of processing on seed oil of *Simarouba glauca*(DC): an underutilized plant", **Journal Food Sci Technology 51(7), 1349–1355.**

Hamzat, K.O., and Clarke, B., 1993,"Prediction of oil yield from groundnuts using the concept of Quasi-Equilibrium of oil yield", **Journal of Agricultural Engineering Research 55, 79-87.**

Herak, D., Kabutey, A., Divisova, M., and Svatonova, T., 2012,"Comparison of the mechanical behaviour of selected oilseeds under compression loading", **Not bot horticulture grobo 40(2), 227-232.**

Jena, K. S., Behera, S., and Rao, Y. R., 2003,"Studies on mechanical expression of Simarouba glauca kernels", **Journal of Oilseeds Research 20(2), 324-326.**

Joshi, J., and Hiremath, S., 2000,"Simarouba: a potential oilseed tree", **Current Science 78 (6), 694-697.**

Khan, L. M., Hanna, M. A., 1983,"Expression of oil from oilseeds – A Review. **Journal of Agricultural Engineering Research", 28,495-503.**

Koushki, M., Nahidi, M., and Cheraghali, F., 2015,"Physico-chemical properties, fatty acid profile and nutrition in palm oil", **Journal of Paramedical Sciences (JPS) 6(3), 117-134.**

Mancini, A.,Imperlini, E., Nigro, E.,Montagnese,C.,Daniele, A., Orrù, S., and Buono, P., 2015,"Biological and Nutritional Properties of Palm Oil and Palmitic Acid: Effects on Health", **Molecules 20, 17339-17361.**

Mishra, S.R., Mohanty, M.K., Das, S.P., and Pattanaik, A.K., 2012,"Production of Bio-diesel (Methyl Ester) from Simarouba Glauca Oil, *Res.J.Chem.Sci.*2(5), 66-71.**

Monseur, X., and Motte, J.C., 1983,"Quantitative HPLC analysis of the bitter quassinoid compounds from Simarouba galuca seeds", **J. Chromatogr 264(3), 469–473.**

*Mwithiga, G., and Moriasi, L., 2007,"*A study of yield characteristics during mechanical oil extraction of preheated and ground soybeans", **Journal of Applied Sciences and Research 3 (10), 1146-1151.**

Neagu, A. A., Irina, N., Botez, E., and Geacai, S., 2013, "A physico-chemical study for some edible oils properties", **Ovidius University Annals of Chemistry 24(2), 121-126.**

Ogunsina, B.S.,Olatunde, G.A., and Adeleye, O., 2014, "Effect of pre-treatments on mechanical oil expression from Dika Kernels", **Journal of Agricultural Technology 10(2), 309-319.**

Oyinlola, A. and Adekoya, L.O., 2004,"Development of a Laboratory Model Screw Press for Peanut Oil Expression", **Journal Food Engineering 64, 221-227.**

Patil, M. S., and Gaikwad, D. K., 2011,"A critical review on medicinally important oil yielding plant laxmitaru (*simarouba glauca*dc.)", **J. Pharm. Sci. & Res. 3 (4), 1195-1213.**

Pradhan, R. C., Mishra, S.,Naik, S. N.,Bhatnagar, N., and Vijay, V. K., 2011,"Oil expression from Jatropha seeds using a screw press expeller", **Biosystems Engineering 109,158-166.**

Pradhan, R. C., Naik, S. N., Bhatnagar, N., and Swain, S. K., 2008,"Moisture-dependent physical properties of Karanja (Pongamiapinnata)", **Industrial Crops and Products 28, 155-161.**

Preeti, Khetarpaul, N.,Jood, S. and Goyal, R., 2007,"Fatty acid composition and physico-chemicalcharacteristics of cooking oils and their blends", **J. Dairying, Foods & H.S.26 (3/4), 202-208.**

Rama, R. D., Nanda, S. K., andSastry, K. R., 2003,"Strategies for augmenting potential of vegetable oils as bio-diesels. Tree borne oil seeds as a source of energy for decentralised planning", **Renew Energy Sci Ser XII, 18–41.**

Rout, P. K., Rao, Y. R., Jena, K. S., Sahoo, D., and Ali, S., 2014 "Safety evaluation of Simarouba glauca seed fat", **Journal of Food Science and Technology 51(7), 1349–1355.**

Santosoa,H., and Iryantoa, M. I., 2014, "Effects of Temperature, Pressure, Preheating Time and Pressing Time on Rubber Seed Oil Extraction Using Hydraulic Press", **Procedia Chemistry 9, 248 – 256.**

Severen, M. L., 1953, "Aceituno seed fat", **J. Am Chem Soc. 30, 124–126.**

Sivala, K., Mukherjee, R. K.,andBhole, N. G., 1993, "A Preliminary Study of Rice Bran Oil Expression in a Manually Operated Hydraulic Press",**Journal of Food Engineering20, 215-222.**

Sukumaran, C. R., and Singh, B. P. N., 1989,"Compression of a Bed of Rapeseeds: The Oil-point", **Journal of Agricultural Engineering Research 42, 77-84.**

Weiss, T.J., 1983,"Commercial Oil Sources", In Food Oils and Their Uses, **West port, C.T., AVI Publishing Company Inc., 49-51.**

RESEARCH ROUNDUP

Chickenfatand biodiesel viscosity modification with additives for the formulation of biolubricants

This study by M.C. Hernández-Cruz et al aimed to develop a lubricant from chicken fat and biodiesel, using additives to meet the standards of physicochemical and environmental quality of the ISO 15380-2012.The raw material was extracted directly from chicken skin; using two methods: autoclaving and direct heating, being the latter which generated the higher extraction yield (52.06%) [Fuel, 198, 42-48, (2017)]. Fat purification (physical refining) was performed by degumming, bleaching and fractionation, where in the fat was transformed from a two-phase mixture to a single-phase solution with improved physicochemical characteristics: viscosity, acid value and mainly fatty acids (48.21%) with prevalence of oleic acid. Viscosity modifiers were added in different ratios (EVA and SBS) following a categorical multifactorial experimental design. As a result, fat mixed with EVA 3 and 4% generated products with similar physicochemical properties to a commercial lubricant, i.e. kinematic viscosity at 40 °C and 100 °C was 108.47 to 174.78 and 20.65 to 27.47 mm2/s, respectively. Biodegradability of formulations were estimated with the BOD5/COD to give a value of 0.6 showing that the product is biodegradable. Thermogravimetrical analysis were done and results demonstrate that thermogravimetrical characteristics are improved if are compared with those of mineral lubricants.Results from this work show that chicken fat is a viable alternative to formulate biolubricants with physicochemical and thermic characteristics to those from commercial lubricants with the advantage of coming from a residual feedstock and being biodegradable.

Assessment of greenhouse gases (GHG) emissions from the tallow biodiesel production chain including land use change (LUC)

Economic uncertainties and environmental constraints regarding fossil fuels have encouraged initiatives for renewable energy sources and assessment of their life cycle impacts. Brazil ranks second worldwide in biodiesel production, despite the relatively recent organization of its national chain, marked by the creation of the National Program for Biodiesel Production and Use (PNPB). The Central-West region is responsible for the largest share of biodiesel production (44.4%) and the largest cattle slaughter (37.5%). In this scenario, beef tallow has great potential for expansion of biodiesel production, since it is a byproduct of the chain that, when not properly disposed, presents a considerable environmental burden. Victor Paulo Peçanha Esteves et al presents a method for assessing environmental performance that integrates life cycle assessment (LCA) with land use change (LUC) for analysis of the tallow biodiesel production chain[Journal of Cleaner Production, 151, 578-

591, (2017)]. The results are given in terms of increment in annual greenhouse gases (GHG) emissions per hectare related to local tallow biodiesel. The system's boundary covers a representative major cattle farming area in Central-West Brazil. For the LCA segment of the method, five inventory allocations were considered: (i) without allocation, (ii) mass, (iii) market value, (iv) energy and (v) an "average allocation", calculated as the mean of mass, market value and energy. The last one is a novel approach proposed in this work, aggregating all the others, which separately result in under or over estimation of impacts. Using the "average allocation", the increment in annual GHG emission per hectare from tallow biodiesel production, is 43.2 kg CO2eq ha−1 y−1. This value is 17% less than the emission increment due to soybean biodiesel (50.2 kg CO2eq ha−1 y−1). LUC is responsible for 96% of the emission assessed, which demonstrates the importance of including LUC assessment in life cycle assessment of tallow biodiesel. According to the sensitivity analyses performed, changes from crop to pasture have superior environmental performance among the investigated options. Land use management is essential to preserve the remaining natural areas, making tallow biodiesel more sustainable.

The production of biodiesel using residualoilfrom palmoilmill effluent and crude lipase fromoilpalm fruit as an alternative substrate and catalyst

Biodiesel production using residual oil from palm oil mill effluent (POME) and crude lipase from oil palm fruit as the substrate and catalyst had a high biodiesel yield (92.07 ± 1.04%) under optimal conditions. POME is considered as an alternative source for oil because it contained high oil and grease content (5569.82 mg/L). Oil was extracted from POME by Saowakon Suwanno et al by the soxhlet method using a mixture of hexane, methanol and acetone. Eighty percent of residual oil (4455 mg/L) was recovered from POME [Fuel, 195, 82-87, (2017)]. Biodiesel production from crude lipase catalyst is an alternative method that is simple to perform and can be done at a low investment cost. In addition, biodiesel from residual oil using crude lipase catalyst was characterized according to ASTM standards. Most properties of biodiesel from crude lipase are acceptable, according to Thai biodiesel and ASTM standards. Low free fatty acid (0.07%) content was observed in enzymatic biodiesel. A high cloud point (10–13 °C) and cetane number (59.0–60.0) were also illustrated since a high cetane number is an important property used to qualify high quality biodiesel, POME biodiesel may possibly be used as a sole biofuel or blended with fossil fuels.

Microencapsulation of palm oil by complex coacervation for application in food systems

Josiane K. Rutz et al aimed at microencapsulating palm oil,

containing high carotenoid content, with chitosan/xanthan and chitosan/pectin, using the complex coacervation method, followed by atomization and lyophilization [Food Chemistry, 220, 59-66, (2017)]. The DSC technique was used to confirm the encapsulation. The atomized microparticles had spherical shape and irregular size, and the lyophilized microparticles had irregular shape and size. Lyophilization resulted in lower carotenoids losses, and higher yield and encapsulation efficiency. In addition, the release profile in both water and gastrointestinal fluid was satisfactory. Prior to their application in food, a greater percentage of carotenoids was released in the fluid that simulates gastrointestinal conditions; however, the compounds were degraded after their release. In this case, the chitosan/pectin microparticles showed the best release profile. After processing, the release was lower and the released compounds were not degraded. Thus, the chitosan/xanthan microparticles showed the best potential for practical application, particularly, in yogurt preparation.

Non-catalytic conversion of glycerol to syngas at intermediate temperatures: Numerical methods with detailed chemistry

Glycerol is available in high volumes and at low costs as a byproduct of bio-diesel production. While combustion characteristics are poor, it is appealing to investigate potential reforming processes to recover its hydrogen and carbon in the form of synthesis gas, i.e. a combustible mixture of hydrogen, carbon monoxide, methane and other small hydrocarbon species. Mohsen Ayoobi and Ingmar Schoeg study pursues a non-catalytic approach, where reactions occur in the gas-phase at elevated temperatures favored by chemical kinetics [Fuel, 195, 190-200, (2017)]. Detailed glycerol reaction chemistry involves many species and reactions, which makes a careful selection of numerical approaches critical. In this work, Eulerian and Lagrangian viewpoints for numerical calculations of a non-catalytic reforming process at intermediate temperatures are studied. All approaches are validated by propane partial oxidation, where non-catalytic experimental results are available in literature. Testing the numerical approaches for a wide range of operating conditions, it is illustrated that the Lagrangian approach outperforms other models in terms of efficiency. Using a transient zero-D Lagrangian technique, glycerol reforming characteristics are discussed at various wall temperatures and mixture conditions. The impact of fuel stoichiometry is investigated based on the oxygen ratio, which is a metric for mixture stoichiometry that accounts for the amount of oxygen bound in the fuel molecules. Results clearly indicate that wall temperatures higher than 1173 K and oxygen ratios in the range of 0.3–0.45 represent conditions that are favorable for glycerol reforming. It is further shown that excess methanol – a commonly found contaminant in crude glycerol – does not affect the reforming performance. As there is a lack of information on non-catalytic glycerol reforming in literature,

qualitative comparisons between non-catalytic (from this work) and catalytic (from literature) glycerol reforming are discussed.

Determination of phospholipids in soybean lecithin samples via the phosphorus monoxide molecule by high-resolution continuum source graphite furnace molecular absorption spectrometry

Laís N. Pires et al present a method for determining phospholipids in soybean lecithin samples by phosphorus determination using high-resolution continuum source graphite furnace molecular absorption spectrometry (HR-CS GF MAS) via molecular absorption of phosphorus monoxide [Food Chemistry, 225, 162-166, (2017)]. Samples were diluted in methyl isobutyl ketone. The best conditions were found to be 213.561 nm with a pyrolysis temperature of 1300 °C, a volatilization temperature of 2300 °C and Mg as a chemical modifier. To increase the analytical sensitivity, measurement of the absorbance signal was obtained by summing molecular transition lines for PO surrounding 213 nm: 213.561, 213.526, 213.617 and 213.637 nm. The limit of detection was 2.35 mg g−1and the precision, evaluated as relative standard deviation (RSD), was 2.47% (n = 10) for a sample containing 2.2% (w/v) phosphorus. The developed method was applied for the analysis of commercial samples of soybean lecithin. The determined concentrations of phospholipids in the samples varied between 38.1 and 45% (w/v).

Synthesis of Methyl Decanoate Using Different Types of Batch Reactive Distillation Systems

Methyl decanoate (MeDC) is a fatty acid methyl ester (FAME) and is an important chemical compound with global production of 31 million tons per year. However, synthesis of methyl decanoate (MeDC) via esterification of decanoic acid (DeC) with methanol by reactive distillation is operationally challenging due to the difficulty of keeping the reactants together in the reaction zone; methanol being the lightest component in the mixture can separate itself easily from the other reactant deteriorating significantly the conversion of DeC using either a conventional batch or continuous distillation column. This is probably the main reason for not applying the conventional route to MeDC synthesis. Whether a semibatch distillation column (SBD) and the recently developed integrated conventional batch distillation column (i-CBD) offer the possibility of revisiting such chemical reactions for the synthesis of MeDC is the focus of this paper by Dhia Y. Aqar et al. The minimum energy consumption (Qtot) as the performance measure is used to evaluate the performances of each of these reactive column configurations for different ranges of methyl decanoate purity and the amount of product [Ind. Eng. Chem. Res, 2017, 56, pp 3969–3982,

(2017)]. It is observed that the use of i-CBD column provides much better performance than the SBD column in terms of the production time and the maximum energy savings when excess methanol is used in the feed. However, the SBD column is found to perform better than the i-CBD column when both reactants in the feed are in equal amounts. Also, the optimization results for a given separation task show that the performance of a two-reflux-interval strategy is superior to the single-reflux interval in terms of operating batch time, and energy usage rate in the SBD process at equimolar ratio.

Steam Deacidification of High Free Fatty Acid in Jatropha Oil for Biodiesel Production

Although non-edible oil feedstocks are available at a lower price than edible oil feedstocks, their high free fatty acid (FFA) content hinders their direct utilization in the production of biodiesel by alkali-catalyzed transesterification [Energy Fuels, 31, pp 6206–6210, (2017)]. In this study, the steam deacidification process has been employed by Godlisten G. Kombe and Abraham K. Temu in reducing the FFA of crude Jatropha oil before alkali-catalyzed transesterification . The response surface methodology (RSM) established on the central composite design (CCD) was used to model and optimize the steam deacidification efficiency under two process variables, namely, temperature and amount of steam. The optimum conditions for deacidification efficiency of 98.74% were found to be the temperature of 235 °C and the amount of steam of 3.4% (w/w) of the feedstock. These conditions reduce the high FFA of crude Jatropha oil from 4.54 to 0.09%, which is below 1% recommended for base-catalyzed transesterification. The deacidified crude Jatrophaoil was then transesterified using a homogeneous base catalyst and gave a conversion of 97.45%. The tested fuel properties of biodiesel, such as viscosity at 40 °C, acid value, gross calorific value, iodine value, fatty acid methyl ester (FAME) content, and density at 15 °C, were found to be comparable to those of ASTM D6751 and EN 14214 standards.

Effect of dietary pomegranate seedoilon laying hen performance and physicochemical properties of eggs

Renata B. Kostogrys et al determined the effects of pomegranate seed oil, used as a source of punicic acid (CLnA) in the diets of laying hens, on the physicochemical properties of eggs[Food Chemistry, 221, 1096-1103, (2017)]. Forty Isa Brown laying hens (26 weeks old) were equally subjected to 4 dietary treatments (n = 10) and fed a commercial layer diet supplying 2.5% sunflower oil (control) or three levels (0.5, 1.0 and 1.5%) of punicic acid in the diets. After 12 weeks of feeding the hens, eggs collection began. Sixty eggs – randomly selected from each group – were analysed for physicochemical properties. Eggs naturally enriched with CLnA preserve their composition and conventional properties

in most of the analysed parameters (including chemical composition, physical as well as organoleptic properties). Dietary CLnA had positive impact on the colour of the eggs' yolk, whereas the hardness of hard-boiled egg yolks was not affected. Additionally, increasing dietary CLnA led to an increase not only the CLnA concentrations, but also CLA in egg-yolk lipids.

'Biofuel parameter dependence on wastefats fatty acids profile

Many studies have focused on biofuel development from non-food biomass. Second generation biofuels (2G) manufactured from waste/recycled greases and animal fats are one of the alternatives to the first generation (1G) plant oil-based biofuels. In this study, the 2G biofuel parameter dependence on waste fats' fatty acids profile was examined by W. Golimowski et al. The methyl esters parameters included density, viscosity and cold filter plugging point (CFPP); and the biofuels used included waste cooking oil (WCO) and waste animal fat (WAF) obtained through low temperature one step trans-esterification process[Fuel, 197, 482-487, (2017)]. Purified and dehydrated samples came from various batches around Poland. Each sample's animal fat content profile was obtained through gas chromatography and acid value method. The fats were transesterifcated at 60 °C with methanol 1:9 (mole/mole) and KOH 1% (m/m) catalyzer. The coefficients of reaction efficiency, viscosity as a function of temperature, density at 15 °C and cold filter plugging point were obtained. Their cause and effect dependence on fat acid's content was evaluated based on correlation coefficient (CC) values. The relative standard deviation (RSD) at 38% pointed to nonhomogeneous content of waste fats. The source of fats had no significant influence on the reaction efficiency, with 0.98 ± 0.015 kg biofuel per 1 kg of waste fat yield. The kinetic viscosity of the biofuels' samples conformed to the EN14214 norm only with two in thirty cases. The dependence of viscosity, density and CFPP on fat acids' profile were confirmed only for a few of studied biofuels.

Transesterification of Rubber Seed Oil to Biodiesel over a Calcined Waste Rubber Seed Shell Catalyst: Modeling and Optimization of Process Variables

In the present study, waste rubber seed shell (RSS) obtained from our previous study was investigated as a plausible solid base catalyst by Samuel Erhigare Onoji et al for the transesterification of esterified rubber seed oil (RSO) to biodiesel [Energy Fuels, 31, pp 6109–6119, (2017]. TGA, XRF, XRD, SEM, and N2 adsorption/desorption analysis (BET) were used to characterize the catalyst. Central composite design (CCD) was employed to design the experiments conducted to study the influence of the process variables (reaction time, methanol/oil ratio, and catalyst

loading) on biodiesel yield. Response surface methodology (RSM) technique, was used to optimize the process, and the quadratic model developed was statistically significant with F-value of 12.38 and p-value (<0.05). The optimum conditions obtained from RSM are as follows: reaction time (60 min), methanol/oil ratio (0.20 vol/vol), and catalyst loading (2.2 g) with a maximum biodiesel yield of 83.11% which was validated experimentally as 83.06 ± 0.013%. Reusability test of the catalyst at optimum conditions shows that the biodiesel yield was over 80% after fourth cycle of usage and the leached Ca2+ ion content of biodiesel was 3.26 mg/kg (ppm). The ester content determined by a precalibrated gas chromatography and the oxidation stability of the biodiesel are 96.7% and 7.8 h, respectively. The characterized biodiesel complied with ASTM D 6751 and EN 14214 biodiesel standards

Encapsulation of tea treeoilby amorphous beta-cyclodextrin powder

An innovative method to encapsulate tea tree oil (TTO) by direct complexation with solid amorphous beta-cyclodextrin (β-CD) was investigated by Meena Shrestha et al. A β-CD to TTO ratio of 90.5:9.5 (104.9 mg TTO/g β-CD) was used in all complexation methods [Food Chemistry, 221, 1474-1483, (2017)]. The encapsulation was performed by direct mixing, and direct mixing was followed by the addition of water (13–17% moisture content, MC) or absolute ethanol (1:1, 1:2, 1:3 and 1:4 TTO:ethanol). The direct mixing method complexed the lowest amount of TTO (60.77 mg TTO/g β-CD). Powder recrystallized using 17% MC included 99.63 mg of TTO/g β-CD. The addition of ethanol at 1:2 and 1:3 TTO:ethanol ratios resulted in the inclusion of 94.3 and 98.45 mg of TTO/g β-CD respectively, which was similar to that of TTO encapsulated in the conventional paste method (95.56 mg TTO/g β-CD), suggesting an effective solid encapsulation method. The XRD and DSC results indicated that the amorphous TTO-β-CD complex was crystallized by the addition of water and ethanol.

Natural Phosphate Supported Titania as a Novel Solid Acid Catalyst for Oleic Acid Esterification

In the present study, a novel solid acid catalyst based on titanium dioxide (2.5–10 wt %) supported on natural phosphate (TiO2/NP) was prepared by Younes Essamlali et al a sol–gel process, and 10 wt % loaded catalyst was characterized by several physicochemical techniques [Ind. Eng. Chem. Res, 56, pp 5821–5832, (2017)]. The performances of the synthesized catalyst were investigated in esterification of oleic acid with methanol. The catalytic performance was screened under different reaction conditions, namely, loading amount of TiO2, calcination temperature, molar ratio of methanol to oleic acid, reaction temperature, and amount of catalyst. Under optimal conditions, the catalyst loaded with 10 wt % TiO2 and

calcined at 800 °C showed the highest oleic acid conversion of 87%. The catalyst showed a good stability under high reaction temperature and can be reused without severe loss of activity. As a versatile application, the TiO2(10)/NP catalyst exhibits a good ability for the esterification of free fatty acids in a highly acidic feedstock.

Tunable volatile release from organogel-emulsions based on the self-assembly ofβ-sitosterol andγ-oryzanol

A current challenge in the area of food emulsion is the design of microstructure that provides controlled release of volatile compounds during storage and consumption. Here, a new strategy by Xiao-Wei Chen et al addressed this problem at the fundamental level by describing the design of organogel-based emulsion from the self-assembly of β-sitosterol and γ-oryzanol that are capable of tuning volatile release [Food Chemistry, 221, 1491-1498, (2017)]. The results showed that the release rate (v0), maximum headspace concentrations (Cmax) and partition coefficients (ka/e) above structured emulsions were significantly lower than unstructured emulsions and controlled release doing undergo tunable though the self-assembled interface and core fine microstructure from internal phase under dynamic and static condition. This result provides an understanding of how emulsions can behave as delivery system to better design novel food products with enhanced sensorial and nutritional attributes

Microencapsulation of palmoilby complex coacervation for application in food systems

This study by Josiane K. Rutz et al aimed at microencapsulating palm oil, containing high carotenoid content, with chitosan/xanthan and chitosan/pectin, using the complex coacervation method, followed by atomization and lyophilization [Food Chemistry, 220, 59-66, (2017)]. The DSC technique was used to confirm the encapsulation. The atomized microparticles had spherical shape and irregular size, and the lyophilized microparticles had irregular shape and size. Lyophilization resulted in lower carotenoids losses, and higher yield and encapsulation efficiency. In addition, the release profile in both water and gastrointestinal fluid was satisfactory. Prior to their application in food, a greater percentage of carotenoids was released in the fluid that simulates gastrointestinal conditions; however, the compounds were degraded after their release. In this case, the chitosan/pectin microparticles showed the best release profile. After processing, the release was lower and the released compounds were not degraded. Thus, the chitosan/xanthan microparticles showed the best potential for practical application, particularly, in yogurt preparation.

Process modeling of hydrodeoxygenation to produce renewable jet fuel and other

hydrocarbon fuels

The focus of this work by Pei Lin Chu et al is to model the hydrodeoxygenation process to produce renewable jet fuel and co-products from low-input oilseeds, specifically camelina, carinata (non-edible oil) and used cooking oil (UCO), taking into account the fatty acid compositions by incorporating the stoichiometric hydrodeoxygenation reactions [Fuel, 196, 298-305, (2017)] . This methodology provides insight into the effect of feedstock composition and hydrodeoxygenation reactions upon product yields, product distribution, hydrogen consumption and process utilities. The resulting product slates, hydrogen gas and utility demands are specific to each of the camelina, carinata and UCO feedstocks.

The yield of kerosene-range alkanes ranged from 53 to 54% of the incoming oil, with 13–14% diesel range alkanes, 13–15% naphtha, and 7–9% liquefied petroleum gas, depending upon the fatty acid composition. The hydrogen consumption rate ranged from 26 to 30 kg per tonne of incoming oil, depending upon the degree of bond unsaturation. Thermal energy demand is 2.8 GJ/tonne oil when processing used cooking oil, versus 5.2 and 5.7 GJ/tonne of oil for carinata and camelina, respectively, owing to the additional energy required for oil extraction. Electricity demand was 73 kWh/tonne oil for UCO, versus 170 and 227 kWh/tonne oil for carinata and camelina.

Physicochemical characteristics of the cold-pressed oil obtained from seeds of Fagus sylvatica L.

A physicochemical characteristic of the cold-pressed oil obtained from seeds of common beech (Fagus sylvatica L.) has been presented by Aleksander Siger et al . This plant may be considered as unconventional oilseeds crops because of relatively high content of fat (27.25%) [Food Chemistry, 225, 239-245, (2017)]. The analyzed beech seeds oil has been classified as oleic-linoleic acids oil with more than 76% percentage share of those species. Beech seeds oil contains 4.2% of gamma-linolenic acid (GLA). Unique characteristic is the high content of γ-tocopherol (75.4 mg/100 g) and δ-tocopherol (34.05 mg/100 g). γ-Tocopherol is effective scavengers of reactive nitrogen species and prevents DNA bases nitration, what makes beech seeds oil interesting raw material in the production of cosmetics. Additionally the content of carotenoids, very effective photooxidation inhibitors, is at high level in comparison with other cold-pressed oils. It was demonstrated that PCA analysis may help to determine the authenticity of oil obtained from beech seeds.

Evaluation of Thermo-oxidative Stability of Biodiesel

Biodiesel susceptibility to oxidation is one of the major problems concerning its use as an alternative to diesel fuel. Although well-characterized, the oxidation process cannot be completely prevented since it can be affected by a large number of factors, such as fuel composition, storage conditions, contaminants, temperature, and the presence of air and light. In this work, Elton L. Savi et al propose Fourier transform infrared spectroscopy (FTIR) in association with principal components analysis (PCA) and hierarchical cluster analysis (HCA) as a method for monitoring the extent of oxidation degree of biodiesel in the low rate phase, before the end of the induction period, in which the changes in the physical properties such as viscosity, mass density, and chain composition of the sample remain almost undetectable. A detailed investigation of thermo-oxidation of biodiesel is reported for a mixture of 50/50 (%) of soybean oil and animal fat biodiesels [Energy Fuels, 31, 7132–7137, (2017)]. The biodiesel degradation was accelerated when maintaining the temperature of the sample at 110 °C under constant air flux for different times. Oil stability index, mass density, viscosity, gross caloric value, esters composition, UV–vis, and FTIR spectra were measured in order to analyze the degree of degradation of each sample. The multivariate analysis in the FTIR spectra clearly shows the discrimination of the samples in the first stage of the degradation process. These results could be useful as a method for monitoring the fuel quality during storage, helping fuel producers, suppliers, and users.

A sustainable and eco-friendly fueling approach for direct-injection diesel engines using restaurant yellow grease and n-pentanol in blends with diesel fuel

Yellow grease from restaurants is typically waste cooking oil (WCO) that is free from suspended food particles and with free fatty acid (FFA) content less than 15%. This study by R. Dhanasekaran et al proposes an approach to formulate a renewable, eco-friendly fuel by recycling WCO with diesel (D) and n-pentanol (P) to improve fuel-spray characteristics[Fuel, 193, 419-431, (2017)]. Three ternary blends (D50-WCO45-P5, D50-WCO40-P10 and D50-WCO30-P20) were selected based on the stability tests and prepared with an objective to substitute diesel by 50% with up to 45% recycled component (WCO) and up to 20% bio-component (n-pentanol) by volume. The fuel properties of these ternary blends were measured and compared. The effect of these blends on combustion, performance and emissions of a stationary DI diesel engine was analyzed in comparison with diesel and D50-WCO50 (50% of diesel + 50% of WCO) with and without exhaust gas recirculation (EGR). Results indicated that addition of n-pentanol showed improved fuel properties when compared to D50-WCO50. While viscosity reduced up to 45%, cetane number and density were comparable to that of diesel. Addition of n-pentanol to D50-WCO50 presented improved brake specific fuel consumption (BSFC) for all ternary blends. BSFC of the blend D50-WCO30-P20 was 8.8% higher than diesel at high engine load without EGR. Brake thermal efficiency (BTE) for D50-

WCO30-P20 blend is comparable to diesel due to improved atomization. However it deteriorated by up to 15.7% at 30% EGR. Smoke opacity reduced by up to 13.6% for D50-WCO30-P20 blend without EGR at high engine load. But it aggravated up to 73% at 30% EGR for D50-WCO30-P20 blend. NOx emission increased with increase in n-pentanol content in D50-WCO50 but remained lower than diesel. However increasing n-pentanol content beyond 20% may increase NOx emissions higher than diesel. NOx can be decreased three-fold using EGR. HC emissions increased and CO emissions remained unchanged with increasing n-pentanol in the blends. By adopting this approach, WCO can be effectively reused as a clean energy source by negating environmental hazards before and after its use in diesel engines, instead of being dumped into sewers and landfills.

Putative Markers of Adulteration of Higher-Grade Olive Oil with Less Expensive Pomace Olive Oil Identified by Gas Chromatography Combined with Chemometrics

Hazem Jabeur et al performed to ascertain that extra-virgin olive oil (EVOO) is free of adulteration [J. Agric. Food Chem, 65, pp 5375–5383, (2017)]. For this purpose, refined pomace olive oils (RPOOs) are commonly used for extra-virgin olive oil adulteration and repassed olive oils (ROOs) are used for lampante olive oil (LOO) fraudulent operation. Indeed, fatty acid ethyl esters could be used as a parameter for the detection of EVOO fraud with 2% RPOO. The addition of >10% RPOO to EVOO would be detected by the amount of erythrodiol, uvaol, waxes, and aliphatic alcohols. Moreover, the use of stigmasta-3,5-diene content proved to be effective in EVOO adulteration even at a low level (with 1% RPOO). For the detection of adulteration of LOO with >5% ROO, the sum of erythrodiol, uvaol, and the waxes and esters can be considered as good markers of purity. Using linear discriminant analysis can identify the most discriminant variable that allows a faster and cheaper evaluation of extra-virgin olive oil adulteration by measuring only these variables.

Kinetics of amidation of free fatty acids in jatropha oil as a prerequisite for biodiesel production

Owing to the growing demand for transportation fuel, enormous efforts are being carried on development of alternate fuels mainly biodiesel from various renewable sources. Different pretreatment methods are adopted for the preparation of biodiesel, major one of the them is the removal of free fatty acids (FFA). Literature reveals esterification as an essential unit process for the reduction of FFA by conversion into its respective esters. In this study, FFA present in jatropha oil were reduced by amidation reaction using monoethanolamine for use in biodiesel by Hari Priya Das et al . The by-product obtained is fatty acid amide. The fatty acid

amide obtained was separated from the feedstock by filtration or centrifugation. This pre-treated oil can be directly transesterified for the preparation of biodiesel without undergoing any process step for removal of unreacted amine [Fuel, 196, 169-177, (2017)]. Also, the reaction kinetics of jatropha oil with monoethanolamine was studied with batch experiments at 34–64 °C and at molar ratios of FFA-monoethanolamine varying from 1:0.5 to 1:2 with different speeds of agitation. Based on the experimental results, 1:1.5 FFA-monoethanolamine molar ratio at 34 °C and 550 rpm gave maximum reduction in free fatty acids. The effect of reaction conditions such as temperature and molar ratio on the kinetics has been studied. Observed reaction rate data was fitted to the regression technique. Estimated kinetic model reaction rate constants and equilibrium constant were fitted to the Arrhenius and van't Hoff equations respectively. The deacidified jatropha oil was transesterified by conventional method and was characterized for its physico-chemical properties.

Novel Reactor for Exothermic Heterogeneous Reaction Systems: Intensification of Mass and Heat Transfer and Application to Vegetable Oil Epoxidation

A novel reactor for exothermic heterogeneous reaction systems was developed by Zhenyu Wu et al and used in a vegetable oil epoxidation process [Ind. Eng. Chem. Res, 56, pp 5231–5238, (2017)] . When hydrodynamic cavitation is coupled with a static mixer, both mass and heat transfer in the reactor can be intensified effectively. The Sauter mean diameter of water/oil dispersion was 8.90 μm under hydrodynamic cavitation conditions with a relatively low inlet pressure (2.5 bar) as compared to 60.33 μm for conventional stirring approach at 500 rpm. The epoxidation temperature variation was controlled within ±1 °C even when the H_2O_2 was added at once, whereas the temperature rise was up to 19 °C in a stirred-tank reactor. The use of this reactor results in decreased reaction time and a simpler and safer process, with final products having quality similar to that obtained in a traditional process.

Low temperature glycerol steam reforming on bimetallic PtSn/C catalysts: On the effect of the Sn content

Steam reforming of glycerol to produce syngas or H2-enriched streams is a promising route that has caught the attention of many researchers around the world. This reaction is typically carried out over metal-based catalysts supported on stable materials. Herein Laura Pastor-Pérez et al report a study on the effect of Sn on the catalytic properties of Pt/C in the aforementioned reaction [Fuel, 194, 222-228, (2017)]. A series of Pt-Sn/C catalysts with different Pt:Sn ratios were prepared and characterized using ICP, H2-TPR, TEM and

XPS techniques, and they were tested in the glycerol steam reforming reaction at 623 K and atmospheric pressure. The best performance was observed for the catalysts with low tin contents. It was found that Sn promoted oxidation reactions and inhibited methanation. Furthermore, the presence of Sn improved the stability of the catalysts when operating at harsher conditions of temperature and glycerol concentration. A promoter effect of Sn hindering platinum sintering and the formation of coke precursors is proposed as the origin of the observed behaviour.

Green synthesis of β-sitostanol esters catalyzed by the versatile lipase/sterol esterase fromOphiostoma piceae

β-sitostanol esters, used as dietary complement for decreasing cholesterol absorption, have been synthesized at 28 °C via direct esterification or transesterification catalyzed by the versatile lipase/sterol esterase by María Molina-Gutiérrez et al from the ascomycete fungus O. piceae. Direct esterification was conducted in biphasic isooctane: water systems containing 10 mM β-sitostanol and lauric or oleic acid as acyl donors, reaching 90% esterification in 3 h with the recombinant enzyme [Food Chemistry, 221, 1458-1465, (2017)]. The use of molar excesses of the free fatty acids did not improve direct esterification rate, and the enzyme did not convert one of the two fatty acids preferentially when both were simultaneously available. On the other hand, solvent-free transesterification was an extremely efficient mechanism to synthesize β-sitostanyl oleate, yielding virtually full conversion of up to 80 mM β-sitostanol in 2 h. This process may represent a promising green alternative to the current chemical synthesis of these esters of unquestionable nutraceutical value.

Determination of phospholipids in soybean lecithin samples via the phosphorus monoxide molecule by high-resolution continuum source graphite furnace molecular absorption spectrometry

Laís N. Pires et al presents a method for determining phospholipids in soybean lecithin samples by phosphorus determination using high-resolution continuum source graphite furnace molecular absorption spectrometry (HR-CS GF MAS) via molecular absorption of phosphorus monoxide [Food Chemistry, 225,162-166, (2017)]. Samples were diluted in methyl isobutyl ketone. The best conditions were found to be 213.561 nm with a pyrolysis temperature of 1300 °C, a volatilization temperature of 2300 °C and Mg as a chemical modifier. To increase the analytical sensitivity, measurement of the absorbance signal was obtained by summing molecular transition lines for PO surrounding 213 nm: 213.561, 213.526, 213.617 and 213.637 nm. The limit of detection was 2.35 mg g^{-1} and the precision, evaluated as

relative standard deviation (RSD), was 2.47% (n = 10) for a sample containing 2.2% (w/v) phosphorus. The developed method was applied for the analysis of commercial samples of soybean lecithin. The determined concentrations of phospholipids in the samples varied between 38.1 and 45% (w/v).

The effect of microwave pretreatment of seeds on the stability and degradation kinetics of phenolic compounds in rapeseed oil during long-term storage

Storage stability and degradation kinetics of phenolic compounds in rapeseed oil pressed from microwave treated seeds (0, 2, 4, 6, 8, 10 min, 800 W) during long-term storage (12 months) at a temperature of 20 °C was discussed in the current study by Agnieszka Rękas et al. The dominant phenolic compound detected in rapeseed oil was canolol, followed by minor amounts of free phenolic acids and sinapine. The most pronounced effect of seeds microwaving was noted for canolol formation – after 10-min exposure the quantity of this compound was approximately 63-fold higher than in control oil [Food Chemistry, 222, 43-52, (2017)]. The degradation of phenolics during storage displayed pseudo first-order kinetics. Differences in the initial degradation rate (r0) demonstrated significant impact of the period of seeds microwave exposure on the degradation rates of phenolic compounds. Results of the half-life calculation (t1/2) showed that the storage stability of phenolic compounds was higher in oils produced from microwave treated rapeseeds than in control oil.

Barcode DNA length polymorphisms vs fatty acid profiling for adulteration detection in olive oil

Ali Tevfik Uncu et al compared the performance of a DNA-barcode assay with fatty acid profile analysis to authenticate the botanical origin of olive oil [Food Chemistry, 221, 1026-1033]. To achieve this aim, we performed a PCR-capillary electrophoresis (PCR-CE) approach on olive oil: seed oil blends using the plastid trnL (UAA) intron barcode. In parallel to genomic analysis, we subjected the samples to gas chromatography analysis of fatty acid composition. While the PCR-CE assay proved equally efficient as gas chromatography analysis in detecting adulteration with soybean, palm, rapeseed, sunflower, sesame, cottonseed and peanut oils, it was superior to the widely utilized analytical chemistry approach in revealing the adulterant species and detecting small quantities of corn and safflower oils in olive oil. Moreover, the DNA-based test correctly identified all tested olive oil: hazelnut oil blends whereas it was not feasible to detect hazelnut oil adulteration through fatty acid profile analysis. Thus, the present research has shown the feasibility of a PCR-CE barcode assay to detect adulteration in olive oil.

MEMBERSHIP OF

OIL TECHNOLOGISTS' ASSOCIATION OF INDIA

There are seven categories of Membership:

- Patrons
- Honorary Fellows
- Life Members
- Corporate Members
- Fellow Members
- Affliate Members
- Student Members

For details, see *www.otai.org*

Journal of Lipid Science and Technology
(Formerly The Journal of the Oil Technologists' Association of India)

ADVERTISEMENT TARIFF

Back Cover (Multi-color)   Rs 35,000/- per insertion (Rs 1,00,000/- per four insertions)
Special Insertion (Multi-color) Rs 35,000/- per insertion (Rs 1,00,000/- per four insertions)
Inside Cover (Multi-color)   Rs 25,000/- per insertion (Rs   75,000/- per four insertions)
Full Page (Multi-color)   Rs 35,000/- per insertion (Rs 1,00,000/- per four insertions)
Full page (Black & White)   Rs 12,000/- per insertion (Rs   40,000/- per four insertions)
Half page (Black & White)   Rs 8,000/- per insertion (Rs   25,000/- per four insertions)

MECHANICAL DATA

Frequency of Publication	:	Quarterly
Overall size	:	28 cms x 21.5 cms
Print area	:	23 cms x 17.5 cms
No. of columns	:	Two
Paper	:	Art paper

All correspondence to:

Dr. R. P. Singh
Ex-Director
H.B.T.I., Kanpur-208002
Mo.: + 91- 9415405642
Phone: + 91- 9721456005
Correspondence Address:
7/105-E, Ratan Kunj, Villa-3,
Swaroop Nagar, Kanpur-208002
E-mail: journalotai@gmal.com,
editorinchief@otai.org,
rpshbti@rediffmail.com

- Payment is to be made in advance by crossed cheque or demand draft in favour of "**Publication Committee, Oil Technologists' Association of India**" **Payable at Kanpur**. Outstation cheques are not accepted. Please send your cheque / DD along with the advertisement material to The Editor at the above mentioned address.

ADVANCE
Home & Personal Care Ltd.

T: +91 11 25060804
F: +91 11 25068604
A: 511/2/1. Rajokri, New Delhi 38
globalsales@advancegroup.biz

Home Care

Dish Wash:
Liquids
Powders
Bars
Gels
Rinse Agents

Cleaners:
Floor
Glass
Toilet
Hard Surfaces
De-odorants

Personal Care

Face Wash
Hand Wash
Body Wash
Toilet Soaps

Shampoos
Hair Condiioners
Hair Oils
Tooth Pastes
Talcum Powders

Fabric Care

Laundry Powders
Laundry Liquids
Laundry Bars

Fabric Softners
Stain Removers
Oil Based
Laundry Bars

A formidable contract-manufacturing partner
Providing manufacturing as a service
Manufacturing HPC products since 1939
Leaders in formulation and manufacturing technology
Excellence in operations management
Pan India presence for logistic and fiscal advantages
Enabling brand owners to focus on their core

Reliancefresh   bharti WAL*MART   VISHAL MEGA MART   spencer's   SRS VALUE BAZAAR

MUEZ HEST
Concept to Performance

A LEADING TECHNOLOGY PROVIDERS & TURNKEY PLANT & MACHINERY SUPPLIERS

OFFERING ENERGY EFFICIENT & ENVIRONMENT FRIENLDY PROJECTS GLOBALLY

EXTRACTION

- PRE - TREATMENT
- EXTRACTION
- DISTILLATION
- DESOLVENTIZATION

OLEOCHEMICALS

- FAT SPLITTING
- GLYCERINE DISTILLATION
- PURIFICATION / EVAPORATION
- TRANSESTERIFICATION

REFINING

- ❑ PHYSICAL
- ❑ CHEMICAL
- DEGUMMING
- BLEACHING
- WINTERIZATION
- DE-WAXING
- DEODORIZATION
- FRACTIONATION

FAT MODIFICATION

- ESTERIFICATION
- INTERESTERIFICATION
- HYDROGENATION

VALUE ADDED PRODUCTS

- LECITHIN
- MARGARINE
- BAKERY SHORTENING

MUEZ-HEST INDIA PRIVATE LIMITED

230 & 231, Blue Rose Industrial Estate., W.E. Highway, Borivali (East), Mumbai - 400 066, INDIA.
Tel/Fax: +91 22 2854 1758 / 28701752, Visit us:- www.muezhest.com, Email: info@muezhest.com